

UCSF

UC San Francisco Electronic Theses and Dissertations

Title

Mechanisms that determine the ordered degradation of APC/C substrates in mitosis

Permalink

<https://escholarship.org/uc/item/4vd1v4hc>

Author

Lu, Dan

Publication Date

2014

Peer reviewed|Thesis/dissertation

Mechanisms that determine the ordered degradation of
APC/C substrates in mitosis

by

Dan Lu

DISSERTATION

Submitted in partial satisfaction of the requirements for the degree of

DOCTOR OF PHILOSOPHY

in

BIOPHYSICS

in the

GRADUATE DIVISION

of the

UNIVERSITY OF CALIFORNIA, SAN FRANCISCO

Copyright 2014

by

Dan Lu

ACKNOWLEDGEMENTS

Graduate school was a pursuit for science, and more importantly an endeavor to grow both as a scientist and as a person. I am extremely grateful for all the people who shared this journey with me and gave me inspiration, encouragement, constructive criticism and room to stumble and learn.

I came to the US from a different continent. I was clumsy with the language and new to the culture. The whole Tang Lab helped me settle down and was my shelter. Genevieve Erwin, Joanna Lipinski and my other iPQB classmates showed me the ropes and have since been great friends. Andrew Horwitz was the nicest rotation mentor, and Molly Darragh was the nicest graduate mentor one can possibly ask for. I also had a wonderful time rotating in the Lim Lab, Weiner Lab, Tang Lab and Morgan Lab. I will forever be grateful for all their help and support in the most challenging transition I have been through.

I owe a lot to my faculty mentors David Morgan, Chao Tang and Wendell Lim for their guidance and for being great role-models. Chao is always positive and encouraging, however rough the time was. He also strongly believes in collaborative approaches and open communication for the advancement of science. Dave deeply cares about his students, postdocs, staff and everyone around him. He has the amazing ability to tailor his mentorship for each person and help them grow in the best way possible. Dave and Chao gave me the space for trial and error, and they were always there when I hit the wall and needed guidance. I also took many weeks-long vacations to visit my family in China, and they never even frowned. I couldn't ask for better PIs. Without Wendell, I would not have been able to pursue my passion and receive the training I had. He is always pushing me to look further and do better. His vision on the bleeding edge of scientific discovery has always been astounding. I also want to thank Orion Weiner,

Hana El-Samad, Susan Miller and Matt Jacobson. Orion and Hana are always generous with their time and willing to mentor young scientists, even when they were not in my committees. It was always helpful talking to Sue about life outside research in her welcoming office. Matt centers the Biophysics graduate program around the students, and is always looking for suggestions and improvement. Along with all the faculty members I crossed paths with during my graduate school career, they showed me what it means to be a great scientist – one that excels in research and also has his/her heart in the community. I will always be grateful for and remember what they have taught me.

Biology research is a rough road. I feel very fortunate to get to know (in chronological order) Xili Liu, Chunbo Lou, Wenzhe Ma, Xiaojing Yang, David Booth, Stephen Floor, Jaline Gerardin, Jennifer Hsiao, Gabriel Rocklin, Juliet Girard, Delquin Gong, Jacob Stewart-Ornstein, Heather Eshleman, Scott Foster, Stephen Naylor, Gilad Yaakov, Chia Wu, Alice Thwin, Matilde Galli and Norman Davey. I am constantly inspired by their love for biology, their strength and persistence facing setbacks, and their willingness to share and help others. I am very grateful for their generous and indispensable help along the way. I also greatly enjoyed my time in lab thanks to the wonderful people in Tang Lab, Morgan Lab, El-Samad Lab and Voigt Lab.

I also want to thank Xili for letting me practicing pipetting with her samples, Xiaojing for teaching me Illustrator, Jaline for bringing me the power cord, Jenny for giving me rides, and Rebecca for offering her red couch. And also sharing all the laughs and tears in these six years. Graduate school would have lost a whole layer of warmth without them.

Lastly I would like to thank my parents Yingkun and Xiaohua, Geoff, and my extended family Nancy, Rol and Chris for their endless love, support and trust in me to follow my heart. I also thank them for always reminding me what is most important in life.

Chapter 2 of this dissertation is a reprint of the material as it appears in the Journal of Cell Biology (Vol 207:23-39, 2014). David O. Morgan and Chao Tang directed and supervised the research that forms the basis for the dissertation; Jennifer Y. Hsiao wrote the MATLAB code for data analysis; Norman E. Davey discovered the ABBA motif and its binding site on Cdc20; Vanessa A. Van Voorhis performed the *in vitro* APC ubiquitination assays; Scott A. Foster provided the *in vitro* results of Dbf4 that motivated the *in vivo* follow up.

ABSTRACT

The ubiquitin-protein ligase APC/C controls mitosis by promoting ordered degradation of securin, cyclins, and other proteins. The mechanisms underlying the timing of APC/C substrate degradation are poorly understood. We explored these mechanisms using quantitative fluorescence microscopy of GFP-tagged APC/C^{Cdc20} substrates in living budding yeast cells. Degradation of the S cyclin, Clb5, begins early in mitosis, followed 6 minutes later by the degradation of securin and Dbf4. Anaphase begins when less than half of securin is degraded. The spindle-assembly checkpoint delays the onset of Clb5 degradation but does not influence securin degradation. Early Clb5 degradation depends on its interaction with the Cdk1-Cks1 complex and the presence of a Cdc20-binding ‘ABBA motif’ in its N-terminal region. The degradation of securin and Dbf4 is delayed by Cdk1-dependent phosphorylation near their Cdc20-binding sites. Thus, a remarkably diverse array of mechanisms generates robust ordering of APC/C^{Cdc20} substrate destruction. We then used a combination of experimental and computational approaches to show that competition among substrates does not contribute significantly to their degradation timing. Instead, the timing and rate of degradation is likely to be primarily determined by the interaction between substrates and APC/C^{Cdc20}. The mechanisms above could change the binding affinity between the substrate and APC/C^{Cdc20}, or the catalytic rate once the substrate is bound to APC/C^{Cdc20}. Depending on parameter region, varying these two properties have different impact on substrate degradation dynamics.

TABLE OF CONTENTS

Acknowledgements	iii
Abstract	vi
List of tables	viii
List of figures	viii
Chapter 1.	1
Introduction	
Chapter 2.	5
Mechanisms that determine the order of APC/C substrate degradation	
Chapter 3.	57
Dynamic simulation of substrate degradation	
Chapter 4.	86
Conclusion	
References	88
	vii

LIST OF TABLES

Table 1: yeast strains used in this thesis	85
--	----

LIST OF FIGURES

Chapter 2:

Figure 1. Metaphase-anaphase transition in cells carrying GFP-tagged APC/C substrates.	33
Figure 2. Timing and dynamics of APC/C ^{Cdc20} substrate degradation.	35
Figure 3. Role of the SAC in APC/C ^{Cdc20} substrate degradation.	37
Figure 4. Role of phosphorylation by Cdk1 in APC/C ^{Cdc20} substrate degradation.	39
Figure 5. Contribution of Cdk1-Cks1 to Clb5 early degradation.	41
Figure 6. Contribution of the ‘ABBA motif’ to Clb5 degradation.	43
Figure 7. APC/C substrate degradation timing in yeast and mammalian cells.	45
Figure 8. Control experiment and data processing methods.	47
Figure 9. Role of SAC in APC/C ^{Cdc20} substrate degradation.	49
Figure 10. Role of phosphorylation in APC/C ^{Cdc20} substrate degradation.	51
Figure 11. Design of Clb5 mutants with decreased binding to Cdk1.	53
Figure 12. Role of Cks1 in APC/C ^{Cdc20} substrate degradation.	55

Chapter 3:

Figure 13. Timing of degradation onset for different strains.	73
Figure 14. A dynamic model for APC-substrate interaction.	75
Figure 15. The delay in degradation onset and rate of degradation varies with parameters.	77
Figure 16. Impact of k_c and k_d on T95 and Td.	79
Figure 17. The region where changing k_d significantly influences T95 varies with k_a .	81
Figure 18. Impact of adding a second substrate C.	83

CHAPTER 1. INTRODUCTION

The ability for cells to reproduce by cell division is a fundamental feature of life. It allows cells to grow in number and ensures the passage of genetic material. Faithful and successful cell division is critical to cells and living organisms, as it forms the very basis of almost all aspects of life, such as growth and differentiation. In eukaryotes, the cell division cycle is a complex process that involves a large number of molecular species working cooperatively and coherently together. These molecules need to replicate the entire genome, package them into sister chromatids, then separate them and partition them into the two progeny cells and eventually form two individual cells. Every step relies on the previous steps, and it is critical they happen at the right time in the right order. Amazingly the cell can carry out this whole process seamlessly without any errors.

Behind this remarkable complexity is a well-organized core regulatory network. It has a hierarchical structure with a few master regulators that orchestrate the activity of hundreds of downstream players. The two major types of master regulators are cyclin-dependent kinases (Cdks) and anaphase-promoting complexes/cyclosomes (APC/C). Cdk and APC/C mutually inhibit each other, and the dividing cells alternate between high APC/C, low Cdk activity in G1 phase, and high Cdk, low APC/C activity in S, G2 and M phases. The activity change in Cdk and APC/C sets the overall pace and stage of cell cycle, which drives the activity of downstream proteins and the progression of cell cycle (Morgan, 2007).

Cdks and APC/Cs regulate very different downstream processes. On top of that, the nine Cdk complexes and two APC/C complexes in budding yeast each has their own preferred substrates. For example, G1-Cdk promotes entry into cell cycle, S-Cdk promotes DNA replication, whereas APC/C^{Cdc20} promotes sister-chromatid separation and APC/C^{Cdh1} promotes cytokinesis (Morgan, 2007). As these master regulators become active in a temporal order,

waves of activity of their downstream proteins follows. The second layer of temporal organization comes from the fact that different substrates that are regulated by the same master regulator complex can also become active or inactive in an ordered fashion. This is observed for both Cdk substrates and APC/C substrates (Pines, 2006; Sullivan and Morgan, 2007).

Another important aspect of cell cycle progression is the dynamics of events, which is essential for a successful cell division. A well-characterized example is the S-Cdk Clb5,6-Cdk1 in budding yeast. Its fast activation is required to trigger DNA replications starting from multiple origins simultaneously and is important for maintaining genome stability (Yang et al., 2013). The dynamics of cellular events all boil down to the dynamics of protein activity, which is determined by a combination of reaction rates from all regulatory inputs. In the case of Clb5,6-Cdk1, it is mainly a result of double negative feedback with its inhibitor Sic1, and the rate of Sic1 degradation (Yang et al., 2013).

In fact, timing and dynamics are intimately intertwined in cell-cycle regulation, as dynamics of the previous events determine the timing of the following events. It is thought that the ordered Cdk substrate phosphorylation is due to different specificity by Cdk, and thus the dynamic of Cdk activation directly determines when certain substrates are phosphorylated (Morgan, 2007). Another interesting aspect is that regulation of the same protein actually could potentially modulate both timing and dynamics of its activity (Yang et al., 2013). How these regulatory mechanisms are integrated and differentiated to influence timing and dynamics is still an open question.

We focused on the master regulator APC/C^{Cdc20}, and followed the timing and dynamics of degradation of its substrates. In Chapter 2, we will study the mechanisms behind different degradation timing of its substrates. In Chapter 3, we will dissect how each component of the

APC/C^{Cdc20}-substrate interaction contributes to the timing and dynamics of substrate degradation.

In Chapter 4, we will summarize our findings.

CHAPTER 2.

MECHANISMS THAT

DETERMINE THE ORDER OF

APC/C SUBSTRATE DEGRADATION

Introduction

Cell division is a fundamental biological process governed by a complex network of regulatory molecules, and the key to its success lies in having the right molecules become active (or inactive) at the right time. The regulatory network controlling cell division is hierarchical: a few master regulators, primarily the cyclin-dependent kinases (Cdks) and the anaphase-promoting complex or cyclosome (APC/C), orchestrate the activities of hundreds of downstream proteins and processes (Morgan, 2007). As the activities of the master regulators rise and fall, they also drive changes in the activities of downstream players. One interesting feature of this regulatory system is that downstream components, even when regulated by the same master regulator, can become active or inactive in an ordered fashion, rather than simultaneously (Pines, 2006; Sullivan and Morgan, 2007). To decipher how the master regulators discriminate between their substrates and achieve this ordering is crucial to our understanding of the orchestration of the cell cycle and other complex processes.

The APC/C is a ubiquitin-protein ligase or E3 that governs mitotic events by promoting timely degradation of key mitotic proteins (Barford, 2011; Peters, 2006; Pines, 2011; Primorac and Musacchio, 2013). Together with its early mitotic activator subunit Cdc20, APC/C promotes the degradation of securin, an inhibitor of separase. Separase then cleaves the cohesins that link the sister-chromatid pairs, triggering sister-chromatid separation (Fig. 1A) (Nasmyth and Haering, 2009). APC/C^{Cdc20} also promotes the degradation of S and M cyclins, which lowers Cdk activity. In budding yeast, APC/C^{Cdc20}-dependent separase activation also leads to the activation of Cdc14, a phosphatase that dephosphorylates numerous Cdk substrates (Queralt et al., 2006; Queralt and Uhlmann, 2008; Stegmeier and Amon, 2004). Among these Cdk substrates is the alternative APC/C activator Cdh1, which together with APC/C promotes the degradation of late-

mitotic substrates and drives the completion of mitosis, cytokinesis and entry into G1 (Fig. 1A) (Sullivan and Morgan, 2007).

APC/C^{Cdc20} and APC/C^{Cdh1} each have multiple substrates, which are degraded at distinct times in the cell cycle (Pines, 2006; Sullivan and Morgan, 2007). In the case of mammalian APC/C^{Cdc20}, the substrates Nek2A and cyclin A are degraded in prometaphase, immediately following nuclear envelope breakdown, while securin and cyclin B are degraded in metaphase (den Elzen and Pines, 2001; Geley et al., 2001; Hagting et al., 2002; Hames et al., 2001). Ordered degradation is equally prevalent among APC/C^{Cdh1} substrates in anaphase and G1 (Pines, 2006; Sullivan and Morgan, 2007). It is not clear how the same APC/C complex robustly distinguishes among its substrates and promotes their degradation at different times in the cell cycle.

The timing of APC/C^{Cdc20} substrate degradation in vertebrate cells is influenced by the spindle assembly checkpoint (SAC), which is activated by unattached kinetochores and inhibits APC/C^{Cdc20} activity toward different substrates to varying degrees. Upon SAC activation, kinetochore-localized SAC components stimulate the formation of soluble Mad2-Cdc20 complexes, leading to the formation of the mitotic checkpoint complex (MCC) consisting of Cdc20, Mad2, Mad3 (in yeast) or BubR1 (in vertebrates), and Bub3 (Lara-Gonzalez et al., 2012; Musacchio and Salmon, 2007). The MCC is the major effector of the SAC. It binds to APC/C and strongly inhibits its activity towards securin and cyclin B, while cyclin A and Nek2A can still be degraded in an active checkpoint due to less efficient inhibition by the MCC (Collin et al., 2013; den Elzen and Pines, 2001; Dick and Gerlich, 2013; Geley et al., 2001; Hagting et al., 2002; Hames et al., 2001). When all kinetochores are properly attached to the spindle, the SAC is turned off and the MCC is disassembled to allow APC/C^{Cdc20}-dependent degradation of securin

and anaphase onset. The protein components and mechanisms of the SAC are highly conserved across species. However, even though the SAC plays an essential role in mammalian cell division (Meraldi et al., 2004; Michel et al., 2004; Michel et al., 2001), disabling the SAC in yeast has very little impact on the cell cycle under normal conditions, and the SAC becomes essential only in the presence of spindle defects (Hoyt et al., 1991; Li and Murray, 1991).

The APC/C recognizes its targets through short sequence motifs called the D box or KEN box, which are often found in unstructured N-terminal regions of APC/C substrates (Glotzer et al., 1991; Pflieger and Kirschner, 2000). Both Nek2A and cyclin A are thought to possess extra binding sites for the APC/C, allowing them to bypass or overcome inhibition by SAC proteins. Nek2A employs a C-terminal motif that resembles Cdc20 and Cdh1 C-termini to bind to the APC/C core directly without the need of an activator (Hames et al., 2001; Hayes et al., 2006; Sedgwick et al., 2013). Cyclin A gains additional affinity for the APC/C^{Cdc20} by forming a complex with Cdk and the accessory subunit Cks1 (Di Fiore and Pines, 2010; Wolthuis et al., 2008). Cks1 binds to Cdk and contributes to recognition of Cdk substrates carrying specific phosphothreonines (Brizuela et al., 1987; Hadwiger et al., 1989; Kõivomägi et al., 2013; McGrath et al., 2013; Richardson et al., 1990; Tang and Reed, 1993). There is also evidence that Cks1 binds APC/C directly to promote its phosphorylation by Cdk (Patra and Dunphy, 1998; Rudner and Murray, 2000; Shteinberg and Hershko, 1999). Thus, cyclin A interacts directly with APC/C^{Cdc20} through its D box and also indirectly through Cdk-Cks1.

Modifications of APC/C substrates also influence their ubiquitination by the APC/C (Holt et al., 2008; Singh et al., 2014). Budding yeast securin has two Cdk1 sites near its D box and KEN box, and phosphorylation of these sites inhibits its ubiquitination *in vitro* (Holt et al., 2008; Holt et al., 2009). Cdc14 dephosphorylates these sites *in vitro*. Given that securin degradation

leads to Cdc14 activation indirectly through separase, these results suggested the existence of positive feedback in securin degradation. Although this phosphoregulation of securin by Cdk1 improves the fidelity of sister-chromatid segregation (Holt et al., 2008), it remains unclear how this regulation influences securin degradation rate and timing. Cdk1 sites are also found inside or near the D box of other budding yeast APC/C substrates (Holt et al., 2009), including Dbf4, the activating subunit for Cdc7 (also known as the Dbf4-dependent kinase or DDK). DDK collaborates with S cyclin-Cdk1 to initiate DNA replication (Bell and Dutta, 2002). Dbf4 is an APC/C^{Cdc20} substrate (Ferreira et al., 2000; Oshiro et al., 1999; Sullivan et al., 2008), but it is not clear whether Cdk phosphorylation contributes to its degradation timing or dynamics.

Here we explore how the interplay among the SAC, Cdk1, APC/C^{Cdc20}, and its substrates lays out the path toward the metaphase-anaphase transition in budding yeast, and we dissect the mechanisms responsible for ordered APC/C^{Cdc20} substrate degradation. We used single-cell analyses of fluorescently-tagged proteins to show that APC/C substrates are degraded in a specific order, with early degradation of the S cyclin Clb5 followed by degradation of securin, Dbf4, and then finally the M cyclin Clb2. We also show that the SAC is largely turned off before the degradation of Clb5 and thus does not contribute to the degradation timing of later substrates. Instead, we find that Cdk-dependent phosphorylation of securin and Dbf4 delays their degradation, and we present evidence that Cks1 and a previously undiscovered sequence motif in Clb5 promote early Clb5 degradation. Together our results provide a temporal and mechanistic view of the key regulatory steps leading to the metaphase-anaphase transition.

Results

APC/C substrates are degraded in a defined order

We used fluorescence microscopy and *in silico* synchronization (Clute and Pines, 1999) to analyze the timing and dynamics of APC/C substrate degradation in living yeast cells. We constructed a series of yeast strains in which a single APC/C substrate (Clb5, securin/Pds1, Dbf4, or Clb2) was tagged at its endogenous locus with a C-terminal GFP. In these strains, the spindle-pole body (SPB) component Spc42 was also tagged at its endogenous locus with C-terminal mCherry. Following their duplication in early S phase, SPBs display two distinctive behaviors that serve as useful indices of mitotic timing: first, at the beginning of mitosis, the two SPBs separate from each other and form a short spindle; and second, at anaphase onset, the two SPBs move quickly away from each other as the spindle begins to elongate, which coincides with separase activation and the onset of sister-chromatid separation (Fig. 1B) (Pearson et al., 2001; Straight et al., 1997; Yaakov et al., 2012).

Using spinning-disk confocal microscopy with 30-sec time resolution, we analyzed these fluorescent markers in individual cells in unperturbed, asynchronously proliferating cultures (Fig. 1B). We first measured the time from SPB separation to spindle elongation in single cells as an estimate of the time from mitotic entry to anaphase onset. This time was highly variable from cell to cell, ranging from 15 to 45 min, with a median of 21 min. Thus, following SPB separation, cells display remarkable variability in the timing of APC/C^{Cdc20} activation and anaphase onset. This timing and variability did not change significantly in any of the strains carrying GFP-tagged APC/C substrates (Fig. 2A, one-way ANOVA p -value = 0.47), consistent with the fact that GFP tagging had no effect on the doubling times of all strains (data not shown). We also confirmed that fluorescence imaging had little impact on mitotic duration (Fig. 8A; see

Materials and methods for optimization of imaging conditions).

Next, in each single cell progressing through mitosis, we monitored the degradation of the GFP-labeled substrate relative to the two SPB events (Fig. 1B, 2B). With this information, we could compare different cells by referencing to the same SPB event, allowing us to compare cells with different GFP-tagged substrates, as well as cells from the same GFP-tagged strain (Fig. 2C, D).

Our results revealed sequential degradation of APC/C substrates during mitosis. At 30°C, Clb5 degradation began an average of 10 min after SPB separation and was almost complete when the spindle started to elongate. Degradation of securin and Dbf4 began about 16 min after SPB separation and was less than half complete when the spindle started to elongate. A small fraction of Clb2 was degraded at the time of anaphase onset, but the majority was degraded later in anaphase (Fig. 1B, 2B, C, D). The substrate ordering we observed is consistent with previous results from population measurements (Ferreira et al., 2000; Lianga et al., 2013). The two phases of Clb2 degradation we observed also support previous evidence that Clb2 degradation is initiated by APC/C^{Cdc20} and later completed by APC/C^{Cdh1} (Baumer et al., 2000; Wäsch and Cross, 2002; Yeong et al., 2000).

With single cell measurements, we were also able to observe variations in the population. When cells were synchronized *in silico* with SPB separation, degradation timing of the same substrate was highly variable in different cells, similar to the variability in mitotic timing (Fig. 2C, top panel; see also Fig. 3A, bottom left panel). This accounts for the fact that the first phase of Clb2 degradation was obscured when we averaged the GFP traces over the population (Fig. 2C as compared to Fig. 2D, bottom panels). Thus, the timing of APC/C activation, and thus its substrate degradation, is not closely correlated to the timing of mitotic onset (SPB separation).

On the other hand, when cells were aligned with the onset of spindle elongation, substrate degradation timing was much less variable (Fig. 2D, top panel; see also Fig. 3A, bottom right panel), consistent with the causal relationship between APC/C^{Cdc20} activation and anaphase onset. Compared to Clb5, the timing of securin degradation had a particularly strong correlation with spindle elongation, in agreement with the fact that securin degradation directly leads to sister-chromatid separation and spindle elongation. Interestingly, Dbf4 was not only degraded at the same time as securin, but its degradation timing also strongly correlated with spindle elongation (Fig. 2D, top panel; see also Fig. 10C), suggesting some link in the regulation of their degradation. The first phase of Clb2 degradation also occurred immediately before spindle elongation, similar to the timing of securin and Dbf4 degradation, consistent with it being APC/C^{Cdc20}-dependent (Fig. 2D).

The spindle assembly checkpoint determines the degradation timing of Clb5 but not that of securin

We next pursued the mechanisms underlying the sequential degradation of APC/C^{Cdc20} substrates. To quantify and compare the timing of substrate degradation in each cell, we determined the time point when 50% of the substrate was degraded, and calculated its timing relative to the reference SPB events (Fig. 8B, C; Fig. 3A, bottom panels; see also Materials and methods). Note that substrate degradation dynamics depend on two factors: the timing of degradation onset and the rate of degradation. Our quantification of the time of 50% degradation provides a combinatorial indication of both factors, and is also more robust than measuring the timing of degradation onset given the noise in our GFP signals (Fig. 8C, unsmoothed traces). In most cases, we also calculated the rate constant of degradation by fitting each single-cell GFP

trace to a single exponential decay, and we present these rates in terms of protein half-life (Fig. 3A, insert; Fig. 8D; see also Materials and methods).

In mammalian cells, the SAC is known to influence the timing of APC/C^{Cdc20} substrate degradation. To assess the contribution of the SAC in our system, we disabled the SAC by deleting *MAD2* (Fig. 3A) or *MAD1* (Fig. 9A), either of which is sufficient to abolish SAC activity (Li and Murray, 1991). To our surprise, disabling the SAC caused Clb5 degradation to occur 4 min earlier than in wild-type cells (Student's *t*-test, *p*-value < 0.001) but left securin degradation timing largely unchanged (Figs 3A and S2A). These data suggest that the SAC normally inhibits Clb5 degradation, and that the timing of Clb5 degradation onset in the absence of the SAC likely indicates the time when APC/C^{Cdc20} becomes active, possibly as a result of APC/C phosphorylation by Cdk1 (Kraft et al., 2003; Rudner and Murray, 2000). In addition, the rate of Clb5 degradation in wild-type cells was very similar to that in *mad2Δ* cells, if not slightly faster (Fig. 3A, insert). This suggests that in wild-type cells the SAC is removed abruptly and APC/C^{Cdc20} is fully activated before Clb5 degradation begins.

The yeast SAC is known to be dispensable for growth in normal conditions but becomes essential under spindle stress. One possibility is that the SAC is activated only in cells that need it, and therefore in normal growth conditions the SAC is activated only in a small subset of cells with kinetochore attachment defects. If this were the case, then there would be a subpopulation of cells with delayed Clb5 degradation due to SAC activation. Disabling the SAC would eliminate this subpopulation and reduce the variability in the timing of Clb5 degradation in the whole population. However, our observations were inconsistent with this possibility. Disabling the SAC led to earlier Clb5 degradation in the entire population without a decrease in variability (Fig. 3A and Fig. 9A), supporting the idea that in yeast cells, as in mammalian cells, the SAC

operates in most cells as an integral feature of cell cycle control.

Securin degradation was largely unaffected by deletion of SAC components (Fig.s 3A and 9A), and the timing of anaphase onset was also unchanged (Fig. 9B). These results are consistent with our evidence from Clb5 timing that the SAC is shut off and APC/C^{Cdc20} is activated several minutes before the onset of securin degradation.

Clb5 can be degraded during an active spindle assembly checkpoint arrest

Given that transient SAC activation in a normal cell cycle delays Clb5 degradation, we wondered whether a prolonged SAC activation would fully stabilize it. We thus plated cells on media containing the microtubule poison nocodazole, which prevents spindle formation and thereby produces a sustained SAC signal. We observed collapsed spindles immediately after nocodazole treatment, indicating an active SAC. Interestingly, we also observed that after 1-2 hours in the arrest, cells began to assemble a spindle and progress into anaphase, perhaps because nocodazole was inactivated under our experimental conditions. We thus used spindle reformation as a single-cell timing marker, before which the cells should have an active SAC and after which cells are recovering from the SAC arrest.

Consistent with previous observations made on a population level, an active SAC inhibited Clb5 degradation but did not fully stabilize the protein (Keyes et al., 2008). Clb5 was degraded slowly in a nearly linear fashion (Fig. 3B, before spindle reformation), even though securin was fully stabilized (Fig. 3C, before spindle reformation). Disabling the SAC by deletion of *MAD2* allowed degradation of Clb5 and securin in nocodazole at a normal rate in the absence of a spindle (Fig. 3D). When we shut off *CDC20* expression from a galactose-inducible promoter (Mumberg et al., 1994), Clb5 was fully stabilized in the presence or absence of nocodazole (Fig.

3E) (Keyes et al., 2008), indicating that the slow degradation in nocodazole depended on APC/C^{Cdc20}. We suspect that this slow degradation of Clb5 also occurs in a normal cell cycle, during the brief 4-minute time window after APC/C^{Cdc20} becomes active towards Clb5 (indicated by the onset of Clb5 degradation in *mad2Δ* cells in Fig. 3A) and before the SAC is turned off (indicated by the onset of fast Clb5 degradation in wild-type cells in Fig. 3A). However, because this time window is so short, and Clb5 degradation during an active SAC is so slow, this partial Clb5 degradation is not noticeable in wild-type cells.

All nocodazole-treated cells eventually assembled a spindle and entered anaphase after 1-2 hours on the nocodazole plate. The reassembly of spindles in these cells suggested that escape from the arrest was due to proper bi-orientation of sister chromatids, and thus inactivation of the SAC, rather than checkpoint adaptation (Vernieri et al., 2013). This fortuitous escape from the checkpoint allowed us to make interesting additional observations. Soon after reformation of the spindle, both Clb5 and securin underwent rapid degradation with a rate very similar to that in an unperturbed cell cycle (Fig. 3B, C, after spindle reformation), indicating abrupt activation of APC/C^{Cdc20} upon SAC inactivation, as observed in unperturbed wild-type cells.

Phosphorylation by Cdk1 delays securin and Dbf4 degradation

To further address the mechanisms that determine the differences in the timing of Clb5 and securin degradation, we studied the influence of Cdk1-dependent phosphorylation on securin degradation. Phosphorylation near its KEN and D boxes (Thr27 and Ser71) was shown previously to inhibit securin ubiquitination by APC/C^{Cdc20} *in vitro*, but it was unclear how this phosphorylation influences the rate or timing of securin degradation *in vivo* (Holt et al., 2008). To determine the effects of this phosphorylation, we replaced the endogenous copy of the securin

gene with a mutant encoding securin-2A (T27A, S71A). The securin-2A mutant was degraded 2 min earlier than the wild-type protein (Fig. 4A, p -value < 0.001), revealing that phosphorylation normally delays securin degradation. Interestingly, a larger fraction of securin-2A was degraded at the onset of spindle elongation compared to wild-type securin (Fig. 4B, p -value < 0.001). This delay between securin-2A degradation and spindle elongation compensated for the earlier degradation of securin-2A to result in only a small but reproducible decrease in the time between SPB separation and spindle elongation (Fig. 10A). In addition, securin-2A was degraded at a slightly greater rate than the wild-type protein (Fig. 4A, insert).

Similar results were obtained with Dbf4. We found that Cdk1 inhibited Dbf4 ubiquitination by the APC/C *in vitro*, and the effects of Cdk1 were reversed by the phosphatase Cdc14 (Fig. 4C). Dbf4 has two putative D boxes starting at Arg10 and Arg62. It was previously shown that mutating Arg62 and Leu65 to alanines stabilized Dbf4 *in vivo* (Ferreira et al., 2000), but we found that mutating Arg10 and Leu13 had a more dramatic inhibitory effect on the ubiquitination of the Dbf4 N-terminal fragment by the APC/C *in vitro* (Fig. 10B). Furthermore, Dbf4 is phosphorylated by Cdk1 at Ser11 *in vivo* (Holt et al., 2009), prompting us to make a Dbf4-A mutant in which Ser11 is mutated to alanine. The ubiquitination of Dbf4-A by APC/C was not inhibited by Cdk1 *in vitro* (Fig. 4D). Like securin-2A, Dbf4-A was degraded slightly earlier than the wild-type protein (Fig. 4E). Although the difference was small, it was consistent whether we synchronized cells to SPB separation (Fig. 4E, p -value = 0.035) or to spindle elongation (Fig. 10C, p -value < 0.001). Thus, Dbf4 and securin are governed by similar Cdk1-dependent regulatory mechanisms, perhaps explaining why they are degraded simultaneously and why Dbf4 degradation is strongly correlated with spindle elongation.

DNA damage is also thought to inhibit securin degradation through Chk1-dependent

phosphorylation of securin at several non-Cdk sites (Agarwal et al., 2003; Wang et al., 2001). We deleted *CHK1* in the securin-2A strain and did not observe any effect on the timing of securin-2A degradation (Fig. 10D), suggesting that this branch of the DNA damage response does not have a significant impact on mitotic timing in an unperturbed cell cycle.

Cks1 binding promotes early degradation of Clb5

Our results indicate that securin phosphorylation accounts for only a part of the difference in the timing of Clb5 and securin degradation. We therefore considered the possibility that there is some feature of Clb5 that promotes its early degradation, perhaps by making it a better APC/C^{Cdc20} substrate. First, we replaced the N-terminal 95 residues of Clb5 with the N-terminal 110 residues of securin-2A. These N-terminal regions contain all of the known APC/C^{Cdc20} binding motifs. This Clb5 chimera was degraded only slightly later than wild-type Clb5 (Fig. 11A). We therefore hypothesized that early Clb5 degradation depends primarily on features within the C-terminal region of Clb5, starting from residue 96.

The Clb5 C-terminal region contains the globular domain that binds and activates Cdk1 (Jeffrey et al., 1995). Interestingly, the early SAC-resistant degradation of mammalian cyclin A depends in part on its binding to the Cdk1-Cks1 complex (Di Fiore and Pines, 2010; Wolthuis et al., 2008). Yeast APC/C^{Cdc20} can bind directly to Cks1, and this interaction promotes APC/C^{Cdc20} phosphorylation by Cdk1 (Rudner and Murray, 2000). These results motivated us to test the contribution of Cdk1 and Cks1 to Clb5 degradation. Given their essential functions in cell-cycle progression, we reasoned that any perturbation in Cdk1 or Cks1 would be likely to have ubiquitous effects on multiple cell-cycle processes, in which case it would be difficult to pinpoint the direct role of these proteins in Clb5 degradation. Instead, we analyzed the degradation of a

Clb5 mutant that cannot bind Cdk1. Based on structural homology and conservation in the cyclin family (see Materials and methods and Fig. 11B), we identified four hydrophobic residues (Ile166, Phe169, Phe254, Phe291) at the predicted Clb5-Cdk1 interface (Fig. 11C) and mutated a combination of them to aspartate or arginine. We then assessed their interaction with Cdk1 *in vivo*. Ectopic expression of a stabilized Clb5 protein lacking its N-terminal region (Clb5-ΔN, with residues 2-95 deleted) under control of the *CLB5* promoter is known to be lethal due to excess Clb5-Cdk1 activity (Sullivan et al., 2008). If our mutations disrupted Clb5-Cdk1 binding, then introduction of these mutants into Clb5-ΔN should prevent its dominant lethal effects. Indeed, when these mutants were expressed under the control of the *CLB5* promoter (582 bp upstream of the *CLB5* ORF) in an integration plasmid, we observed improved growth as we increased the number of mutations in Clb5-ΔN (Fig. 11D), even though all mutants had a similar expression level in the cell (Fig. 11E). When we combined three mutations (F169D, F254D, F291D; henceforth the Clb5-3D mutant), the cells grew with a doubling time (85.4±0.2 min) very similar to that of wild-type cells (84.1±0.5 min); adding a fourth mutation (I166D, F169A, F254D, F291D) did not further improve growth (85.6±0.1 min). Furthermore, the Clb5-3D mutant almost completely failed to associate with Cdk1 in cell lysates (Fig. 5A). We therefore used the Clb5-3D mutant for the following experiments.

We expressed Clb5-GFP or Clb5-3D-GFP under the control of the *CLB5* promoter, using an integration plasmid. Both strains retained the endogenous copy of *CLB5* to maintain a normal cell cycle. We found that Clb5-3D displayed two phases of degradation: a slow phase and a fast phase (Fig. 5B). The slow phase displayed a nearly linear rate and was not dependent on Cdc20 (Fig. 12A), and so it likely reflected non-specific degradation of Clb5-3D due to destabilizing effects of the mutations. The fast phase, however, disappeared if we shut off Cdc20 expression

and thus reflected APC/C^{Cdc20}-dependent degradation (Fig. 12A). This fast phase of Clb5-3D degradation was significantly delayed relative to the degradation of wild-type Clb5 (Fig. 5B, p -value < 0.001), suggesting that Cdk1 binding contributes to early Clb5 degradation.

These results are consistent with a role for Cdk1 binding in Clb5 degradation, and this is most likely mediated through Cks1, which binds to both Cdk1 and APC/C (Di Fiore and Pines, 2010; Patra and Dunphy, 1998; Rudner and Murray, 2000; Shteinberg and Hershko, 1999; van Zon et al., 2010; Wolthuis et al., 2008). To directly test the role of Cks1, we fused Cks1 to the C-terminus of Clb5-3D-GFP. The Cks1 fusion rescued the delay in Clb5-3D degradation (Fig. 5B, p -value < 0.001), indicating that Cks1 facilitates early degradation of Clb5.

We also fused Cks1-GFP to the C-terminus of securin-2A and compared degradation of the fusion protein with that of securin-2A-GFP. In both cases, the endogenous copy of securin was replaced to ensure that the cells expressed only one securin variant, the degradation of which would drive sister-chromatid separation. Securin-2A-Cks1 was degraded significantly earlier than securin-2A (Fig. 5C, p -value < 0.001) and at a slightly faster rate. Accordingly, anaphase onset also occurred significantly earlier (Fig. 12B, p -value < 0.001) and sooner relative to Clb5 degradation (Fig. 5C, right panel). Interestingly, as in our earlier observations with securin-2A, more securin-2A-Cks1 was degraded than securin-2A when spindle elongation occurred (Fig. 5D, p -value < 0.001), suggesting that securin degradation is not the sole determinant of anaphase onset.

However, Cdk1-Cks1 binding did not fully explain early Clb5 degradation relative to securin-2A: Clb5-3D was still degraded earlier than securin-2A (Fig. 12C, p -value < 0.005). We suspected that additional mechanisms exist to promote early degradation of Clb5.

The Cdc20-binding ‘ABBA Motif’ contributes to Clb5 degradation in the presence or absence of an activated SAC

A short amino acid sequence motif in the yeast protein Acm1 interacts with the WD40 domain of Cdh1 at a site distinct from the binding sites for the D box and KEN box (Burton et al., 2011; Enquist-Newman et al., 2008; He et al., 2013). Recent studies suggest that a related motif exists in cyclin A and facilitates its early mitotic degradation via APC/C^{Cdc20} (Di Fiore, Davey, and Pines, submitted for publication). Originally called the ‘A motif’, this motif was renamed the ‘ABBA’ motif to reflect its conserved presence in Acm1, Bub1, BubR1, and cyclin A. We tested the possibility that a similar motif exists in Clb5 and helps promote early Clb5 degradation. We performed a motif search in Clb5 homologs from closely-related yeast species of the *Saccharomyces* clan (Davey et al., 2012), and we found a putative ABBA motif at residues 99-105 in Clb5, within a highly conserved region (Fig. 6A).

To test the function of the putative ABBA motif in Clb5, we replaced the key residues Ile102 and Tyr103 with alanines to generate the Clb5-2A mutant. Clb5-2A was degraded significantly later than Clb5 (Fig. 6B, p -value < 0.001), but at a very similar rate (Fig. 6B, insert). We also analyzed a Clb5 mutant (Clb5-2A3D) in which both Cdk1 binding and the ABBA motif were disrupted. The rapid phase of degradation of this mutant now occurred slightly later than the degradation of securin-2A (Fig. 6C).

The ABBA motifs in Clb5 homologs differ from those in Acm1 and cyclin A by having conserved basic residues upstream of the core Ile102 and Tyr103 (Fig. 6A). We wondered whether this was accompanied by differences in the ABBA motif binding site on Cdc20. Based on homology modeling of the Acm1-Cdh1 structure (He et al., 2013), we identified residues on Cdc20 that potentially interact with the ABBA motif, and we compared them to those on Cdh1.

One striking difference was a cluster of acidic residues (Asp311, Asp312, Asp313) in Cdc20 that are absent in Cdh1 (Fig. 6D). If these residues are important for binding to the basic residues in the Clb5 ABBA motif, then replacing the endogenous *CDC20* with a *CDC20-GAG* (D311G, D312A, D313G) mutant should delay wild-type Clb5 degradation but have little impact on Clb5-2A degradation. Indeed, this is what we observed (Fig. 6D, p -value < 0.001 and p -value = 0.8775, respectively).

We confirmed these findings with APC/C-dependent ubiquitination reactions *in vitro*. In reactions with wild-type Cdc20 as the activator, the ubiquitination of Clb5-2A was less efficient than that of wild-type Clb5. Consistent with this result, wildtype Clb5 was less efficiently modified in reactions with the Cdc20-GAG mutant, and ubiquitination of Clb5-2A was similar in reactions with wild-type and mutant Cdc20 (Fig. 6E).

We conclude that the early degradation of Clb5 in a normal cell cycle depends mostly, if not entirely, on Cdk1-Cks1 and the ABBA motif, both of which provide additional binding sites for APC/C^{Cdc20}. We also tested the effect of ABBA motif disruption on Clb5 degradation in nocodazole. Compared to wild-type Clb5, the Clb5-2A mutant was still degraded in a linear fashion but at a significantly slower rate (Fig. 6F). Thus, the ABBA motif also contributes to Clb5 degradation in an active SAC.

Discussion

Our results, together with those from previous single-cell studies, provide a detailed temporal picture of how yeast cells progress towards the metaphase-anaphase transition (Fig. 7). The process begins with inactivation of the SAC, which inhibits APC/C^{Cdc20} activity until all sister-chromatids are properly attached to the spindle. Activated APC/C^{Cdc20} first degrades the S

cyclin Clb5 with an average half-life of 3.4 min. About 6 min later, securin is degraded with an average half-life of 4.7 min. Soon after securin degradation begins, separase is abruptly activated, and only 1 min is required for separase to cleave enough cohesin to promote sister-chromatid separation (Yaakov et al., 2012). By the time of sister-chromatid separation, Clb5 is fully degraded but more than half of securin remains.

The SAC is not essential for yeast viability under normal growth conditions (Hoyt et al., 1991; Li and Murray, 1991), and thus it has not been clear what role, if any, the SAC plays in the normal timing of yeast mitotic regulatory events. Our experiments now reveal that the SAC is activated in most yeast cells as an integral part of progression through mitosis. Compared to the SAC in mammalian cells, however, the yeast checkpoint appears to be inactivated relatively early in mitosis and determines the timing of S cyclin degradation and not that of securin. Our results are consistent with the observation that, in yeast, bi-orientation of sister-chromatids on the spindle begins immediately after spindle assembly and is possibly complete many minutes before anaphase onset (Goshima and Yanagida, 2000; He et al., 2000; Pearson et al., 2001; Tanaka et al., 2000). Thus, the nonessential nature of the SAC may be due, at least in part, to the waiting period between the proper attachment of sister chromatids (and SAC inactivation) and their separation. Even without the surveillance provided by the SAC, the sister-chromatid pairs would normally achieve proper attachment to the spindle minutes before securin degradation triggers their separation.

With the SAC turned off or disabled, we found that the ordered degradation of Clb5, securin, and Dbf4 is established primarily through differences in their interaction with APC/C^{Cdc20}. Cdk1-dependent phosphorylation near KEN and D boxes in securin and Dbf4 can delay their degradation, and this similarity in regulation results in almost simultaneous

degradation of these substrates. We also found that the early degradation of Clb5 depends on two factors that provide additional binding sites for APC/C^{Cdc20}: the interaction of Clb5 with the Cdk1-Cks1 complex and the presence of the ABBA motif in the Clb5 N-terminal region. We still lack a complete mechanistic understanding of how these factors influence the interaction between substrates and APC/C^{Cdc20} inside the cell. They could simply improve substrate-binding affinity for APC/C^{Cdc20}, or they might help orient substrates (or lysines in those substrates) for efficient ubiquitin transfer. They might also provide selectivity for specific subpopulations of APC/C^{Cdc20}. For example, Cks1 is thought to interact with the phosphorylated subpopulation of the APC, which has higher binding affinity for Cdc20 (Rudner and Murray, 2000).

We can only speculate about how differences in binding interactions with APC/C^{Cdc20} are converted to a robust ordering of substrate degradation. One can imagine two possible scenarios that are not mutually exclusive. In a 'threshold' model, APC/C^{Cdc20} activity continues to rise following its initial activation, and efficient ubiquitination of securin or Dbf4 might require a higher level of APC/C^{Cdc20} activity than that of Clb5. Such thresholds could be established by changes in docking interactions between substrates and APC/C^{Cdc20} as mentioned above, as well as by phosphoregulation of APC/C^{Cdc20}. In an alternative 'competition' model, the amount of active APC/C^{Cdc20} is limiting, and substrates compete with each other for APC/C^{Cdc20} binding. In this case, APC/C^{Cdc20} is initially occupied by higher-affinity substrates such as Clb5, and only after destruction of these substrates can efficient securin and Dbf4 ubiquitination begin. Our results seem to argue against this model and are more consistent with a threshold model. For example, when we measured the timing of Clb5-2A degradation, we deleted the endogenous copy of Clb5. If Clb5 competitively inhibited the degradation of lower-affinity substrates, then the prediction would be that destruction of the Clb5-2A mutant would not be delayed because its

Clb5 competitor was absent. A complete understanding of substrate ordering will require more detailed quantitative analyses of APC/C^{Cdc20} activation, phosphoregulation, and localization in the cell.

A major difference between mammalian and yeast cells is that cyclin A is thought to be degraded in the presence of an active SAC and needs to compete with SAC proteins for APC/C^{Cdc20} binding (den Elzen and Pines, 2001; Geley et al., 2001), whereas Clb5 degradation appears to occur just after the SAC is turned off. Interestingly, despite these very different circumstances, the same two mechanisms—Cks1 and the ABBA motif—allow cyclin A and Clb5 to be degraded earlier than other substrates (Di Fiore, Davey, and Pines, submitted for publication; Di Fiore and Pines, 2010; Wolthuis et al., 2008). It was shown recently that the degradation of cyclin A and securin seems to remain sequential in mammalian cells without a functional SAC (Collin et al., 2013). We suspect that in this scenario, the same mechanisms promote cyclin A degradation earlier than that of other substrates.

We found that Clb5, like cyclin A, is degraded in cells with an active SAC, but the rate of degradation was much slower than that in the absence of the SAC (Keyes et al., 2008). This slow degradation depends on Cdc20 and on the ABBA motif, suggesting that this motif is capable of driving some interaction with APC^{Cdc20} even in the presence of an active SAC. We also suspect that Clb5 degradation in the presence of the SAC depends on Cdk1-Cks1 binding, but we could not test this possibility due to the intrinsic instability of our Clb5-3D mutant.

Securin degradation leads to sister-chromatid separation, but the timing of sister separation also seems to depend on other factors. Among the different variants of securin we tested, including the wild-type protein, securin-2A and securin-2A-Cks1, earlier degradation correlated with an increase in the amount of securin that was degraded before anaphase onset.

This could suggest another branch of regulation in the timing of sister-chromatid separation. Indeed, the cohesin subunit Scc1 is phosphorylated by Polo kinase, which increases the rate of cleavage by separase by several fold (Alexandru et al., 2001; Yaakov et al., 2012). One can imagine that when securin is degraded early, and separase is released early, Scc1 is not yet fully phosphorylated and cohesin cleavage will take longer to complete. Consistent with this idea, Scc1 is cleaved more slowly in securin-2A cells than in wild-type cells (Yaakov et al., 2012).

Our results suggest that there is a 9-minute delay between the completion of sister-chromatid bi-orientation (SAC satisfaction) and the initiation of sister-chromatid separation via securin degradation. Does this time delay serve a purpose? One possibility is that the delay allows time for complete Clb5 degradation before anaphase begins. Clb5-Cdk1 phosphorylates numerous specific substrates that have functions in anaphase (Loog and Morgan, 2005), and these functions are inhibited by Cdk1-dependent phosphorylation. These substrates include the spindle stabilizer Fin1 (Woodbury and Morgan, 2007), the spindle midzone organizer Ase1 (Juang et al., 1997; Khmelinskii et al., 2009), the SPB component Spc110 (Kilmartin et al., 1993; Lianga et al., 2013), the late mitotic APC/C activator Cdh1 (Jaspersen et al., 1999; Visintin et al., 1997), and the kinetochore component Cnn1 (Bock et al., 2012; Schleiffer et al., 2012). Several of these proteins are dephosphorylated by Cdc14 (Jaspersen et al., 1999; Khmelinskii et al., 2009; Woodbury and Morgan, 2007). The early degradation of Clb5, which is completed by the onset of anaphase and coincides with activation of Cdc14, may allow earlier and more abrupt activation of these Clb5 substrates and lead to a more efficient and coherent anaphase. Indeed, removing securin phosphorylation, which disturbs the coordination between Clb5 degradation and anaphase onset, was shown to impede spindle elongation and increase chromosome loss (Holt et al., 2008). Stabilized Clb5 has also been shown to slow down spindle elongation (Lianga

et al., 2013) and delay rDNA segregation (Sullivan et al., 2008). There is also recent evidence in mammalian cells that cyclin A destruction before anaphase is important for the stabilization of kinetochore-microtubule attachments (Kabeche and Compton, 2013). Thus, differences in the relative timing of cyclin and securin degradation are likely to make important contributions to the overall orchestration of mitosis.

Materials and methods

Yeast strain construction

All yeast strains were haploid derivatives of the W303 strain (Table 1). Fluorescent protein tagging, gene replacement, and deletion of genes at their endogenous loci were performed using standard PCR-based homologous recombination (Baudin et al., 1993; Goldstein and McCusker, 1999; Jansen et al., 2005; Longtine et al., 1998), while preserving the endogenous promoters. Addition of genes to the genome was done using an integration plasmid at the genomic *TRP1* locus (Sikorski and Hieter, 1989), with promoters as indicated in Table S1, and selected for single-copy integration by PCR and fluorescence intensity.

Fluorescence microscopy

All images were taken with a spinning-disk confocal microscope at the UCSF Nikon Imaging Center with a 60x/1.4 NA oil immersion objective, under the control of Micromanager (Edelstein et al., 2010). The microscope is a Nikon Ti-E inverted microscope equipped with a Yokogawa CSU-22 scanner unit and a Photometrics Evolve EMCCD camera. Illumination was provided by a 50 mW 491 nm laser and a 50 mW 561 nm laser. Imaging sessions were generally 1 h long, or 1.5 h for nocodazole experiments, with 30- or 45-sec time intervals. Z-stacks were taken across 4 μm of distance with 0.5 μm steps for each time point and each channel. Exposure

times for mCherry and GFP channels were below 40 ms for each Z slice.

All yeast cultures were grown and imaged at 30°C. Prior to imaging, yeast cells were grown in synthetic complete media with 2% glucose (SD) for 24 h with serial dilution to maintain OD below 0.4. For imaging, cells were mounted on a 1.5% agarose pad made with SD media, and allowed to continue proliferating on the slide for 40-60 min in a 30°C incubator prior to imaging. For nocodazole experiments, cells were plated onto an agarose pad containing 15 ug/ml nocodazole for 5-10 min prior to imaging. For experiments involving the shutting off of galactose-induced promoters, cells were grown in 2% galactose for 24 h, spinned down and plated onto an agarose pad containing 2% glucose for 5-10 min prior to imaging.

All single cell data in the same plot were taken within the same week. Every strain had two or three repeats each from a different single colony from transformations that generate the strain. Differences between colonies were negligible, and figures show cells from all repeats combined.

Optimization of imaging conditions

To minimize phototoxicity while retaining sufficient temporal resolution and dynamic range of the fluorescent signal, we optimized our imaging conditions in several ways. First, the specific setup of the spinning-disk confocal microscope at the UCSF Nikon Imaging Center allowed much shorter exposure times and more frequent time points than with other microscopes we tested. Second, the yeast nitrogen base in our SD media was a significant source of background fluorescence, and we found that yeast nitrogen base from Sigma-Aldrich had less auto-fluorescence than others. Autoclaving SD media ingredients also raised the auto-fluorescence level, so all media was filtered instead. Third, during the imaging process, we took one frame every 30 or 45 sec, which was just enough to capture the features of the dynamics of

substrate degradation. For fitting of the degradation rate, a 30-sec time interval was the minimum required to obtain enough data points during one degradation event for a good fit. We also took short movies of about 1 h, which covers only one round of mitosis. Last, we used the minimum level of laser intensity and exposure time to generate fluorescent signals that were minimally sufficient for quantification.

Image processing

To quantify GFP intensity at each time point, we first used ImageJ (<http://imagej.nih.gov/ij/>) (Schneider et al., 2012) and its plugin Image5D (<http://rsb.info.nih.gov/ij/plugins/image5d.html>) to average across each z-stack and flatten it to 2D. GFP intensity was then quantified using MATLAB (The MathWorks Inc.) code previously developed in the Tang lab (Yang et al., 2013). Since all of the APC/C substrates we studied were localized to the nucleus, we took the brightest square of 5x5 pixels in the cell as an estimate of the protein level (Fig. 8B). Timing of SPB events was determined based on the temporal 3D positions of the SPB using the mCherry images. SPB separation was defined as the time point when one SPB split into two, and spindle elongation was defined as the time point when two SPBs began to move rapidly away from each other.

Data processing

The time point of 50% substrate degradation in each cell was defined as when GFP intensity was halfway between the maximum and the minimum intensity on a smoothed trace of a degradation event (Fig. 8C). For Clb5-3D strains in which slow degradation occurred prior to the fast degradation by APC/C^{Cdc20}, the maximum intensity was replaced by the intensity right before the fast degradation began, so that the resulting 50% degradation point corresponds to the midpoint of the fast degradation. Determination of the timing of the 50% drop of GFP signal, or

the level of GFP at a certain time point, was carried out with newly developed MATLAB code (Crocker and Grier, 1996). The rate of substrate degradation in single cells was calculated by fitting the fast decreasing section of each GFP trace, spanning at least 7 time points for a robust fit, to a single exponential decay (Fig. 8D) with MATLAB code previously developed in the Tang lab (Yang et al., 2013). Statistical analysis and plotting were carried out in MATLAB and Python (Hunter, 2007; Oliphant, 2007).

Ubiquitination assays *in vitro*

For analysis of APC/C activity with phosphorylated Dbf4 (Fig.s 4C, 4D, S3B), wild-type and mutant Dbf4 substrates, carrying a C-terminal ZZ tag and TEV cleavage site, were translated *in vitro* with TnT Quick Coupled Transcription/Translation Systems (Promega) in the presence of ³⁵S-methionine. Substrates were immobilized on IgG beads and incubated at 23°C for 60 min with purified Clb2-Cdk1 in kinase buffer (25 mM HEPES [pH 7.4], 150 mM NaCl, 10 mM MgCl₂, 1 mM ATP, 5% glycerol). Beads were washed with QAH buffer (20 mM HEPES [pH 7.4], 150 mM NaCl, 1 mM MgCl₂, 10% glycerol) and cleaved with TEV protease to produce soluble radiolabeled Dbf4 substrates. APC/C was purified from lysates of *TAP-CDC16 cdh1Δ* W303 strains by affinity chromatography with IgG beads, followed by elution with TEV protease (Carroll and Morgan, 2002). E1 (Uba1-6His) was expressed in yeast and purified by metal-affinity chromatography (Carroll and Morgan, 2002). E2 (Ubc4-6His) was expressed in bacteria and purified by metal-affinity chromatography (Rodrigo-Brenni and Morgan, 2007). Activator was tagged with an N-terminal ZZ tag and TEV cleavage site and produced with TnT Quick Coupled Transcription/Translation Systems (Promega), followed by purification on IgG beads and TEV cleavage (Foster and Morgan, 2012). E2 charging was performed in the presence of E1 (Uba1, 300 nM), E2 (Ubc4, 50 uM), methyl-ubiquitin (Boston Biochem, 150 uM), and ATP (1

mM) at 23°C for 20 min. APC/C reactions were initiated by mixing APC/C, activator, substrate, and charged E2. Reactions were performed at 23°C for 60 min. Reaction products were separated by SDS-PAGE and visualized with a Molecular Dynamics PhosphorImager.

For analysis of APC/C activity with securin and Clb5 (Fig. 6E), lysate was prepared from a ~300 mg pellet of *TAP-CDC16 cdh1Δ* W303 cells, and APC/C was immobilized on IgG-coupled Dynabeads (Invitrogen) as described (Matyskiela and Morgan, 2009). The final concentration of APC/C in each reaction was ~1 nM. ZZ-tagged substrates were generated *in vitro* with TnT Quick Coupled Transcription/Translation Systems (Promega) in the presence of ³⁵S-methionine, and purified with IgG-coupled Dynabeads and cleaved using TEV protease. E2 charging and ZZ-tagged activator purification were performed as described above. APC/C reactions were initiated by the addition of activator, substrate, and charged E2 to immobilized APC/C, and incubated at 23°C for 30 min. Reaction products were separated by SDS-PAGE and visualized with a Molecular Dynamics PhosphorImager.

Design of Clb5 mutant with a Cdk-binding defect

We first used HOMCO (Fukuhara and Kawabata, 2008) to build homology models of the Clb5-Cdk1 complex based on several available cyclin-Cdk structures, including cyclin B-Cdk2 (2jgz) (Brown et al., 2007), cyclin A-Cdk2 (1jst) (Russo et al., 1996), and cyclin E-Cdk2 (1w98) (Honda et al., 2005). Our initial pool of candidate residues was selected from residues predicted to be at the cyclin-Cdk interface. We then selected the residues for mutation using the following criteria: they should be present at the Clb5-Cdk interface in all of the three homologous structures; they should not participate in intramolecular interactions, so that mutations in those residues are less likely to destabilize Clb5; and they should be conserved in all budding yeast cyclins, which all bind to the same Cdk1 (Fig. 11B). This narrowed the candidates down to four

residues (I166, F169, F254, F291), as shown in Fig. 11C (Pettersen et al., 2004). We then made a number of Clb5- Δ N mutants (with residues 2-95 deleted) (Sullivan et al., 2008) containing a combination of these residues mutated to arginine or aspartate and expressed them under control of the *CLB5* promoter (582 bp upstream of the *CLB5* ORF). Cells expressing either wild-type Clb5- Δ N or Clb5- Δ N with a single mutation of F254D were inviable (data not shown). Clb5- Δ N with double mutations inhibited cell growth more than triple mutations (Fig. 11D). Cells with Clb5- Δ N triple mutations and quadruple mutations all grew at a rate similar to the parent strain without Clb5- Δ N.

To analyze Cdk1 binding to Clb5 mutants, log-phase cells with full-length wild-type or mutant Clb5-GFP expressed under the endogenous *CLB5* promoter were lysed by bead-beating in lysis buffer (50 mM HEPES [pH 8.0], 150 mM NaCl, 1% NP40, 50 mM beta-glycerophosphate, 50 mM NaF, 1 mM DTT, 1 ug/ml leupeptin, 1 ug/ml pepstatin, 1 ug/ml aprotinin, 1 mM PMSF, 10% glycerol, 0.63 mg/ml benzimidazole, 5 mM EDTA). Lysates were incubated with GFP-binding protein (Rothbauer et al., 2008) covalently coupled to sepharose beads (NHS-Activated Sepharose 4 Fast Flow, GE Healthcare) at 4°C for 30 min. The beads were then washed with lysis buffer, and associated proteins were analyzed by western blotting with a mixture of anti-Cdk1 (Cdc2 p34 [PSTAIRE], Santa Cruz sc-53) and anti-GFP (GFP-FL, Santa Cruz sc-8334).

Acknowledgements

We thank Hana El-Samad, Jaline Gerardin, Wendell A. Lim, Xili Liu, Geoff C. Rollins, Jacob Stewart-Ornstein, Orion D. Weiner, Xiaojing Yang, and members of Morgan and Tang labs for inspiring discussions and comments on the manuscript; Kurt Thorn, Alice Thwin and DeLaine Larsen at the UCSF Nikon Imaging Center for their critical help with microscopy; Heather Eshleman, Matilde Galli, and Arda Mizrak for reagents; and Jon Pines and Barbara Di Fiore for sharing results prior to publication.

This work was supported by a fellowship (to D.L.) from the UC Cancer Research Coordinating Committee (CRCC) and by funding from the National Institute of General Medical Sciences (R01-GM097115 to C.T. and R37-GM053270 to D.O.M.).

The authors declare no competing financial interests.

Figure 1

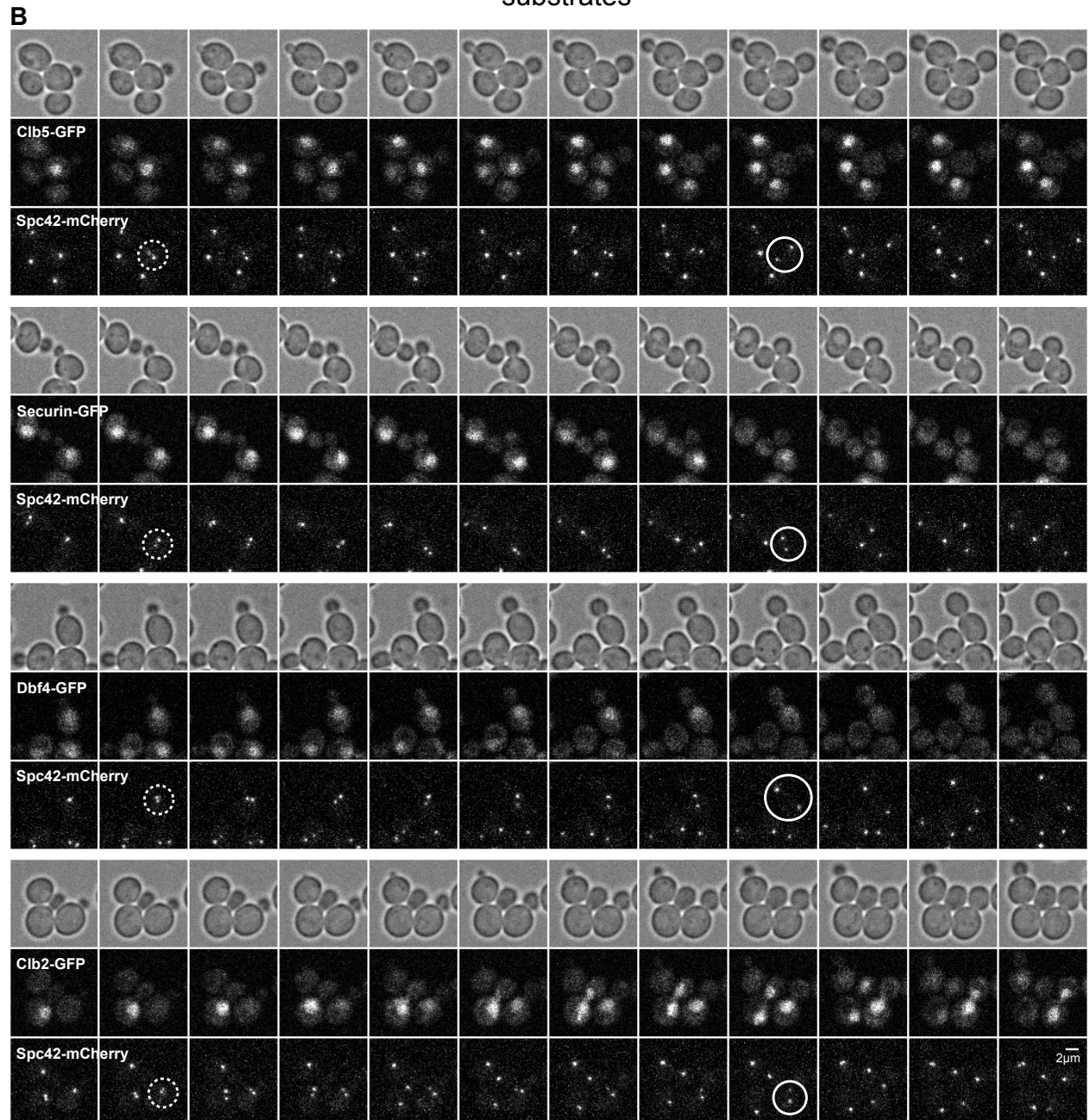
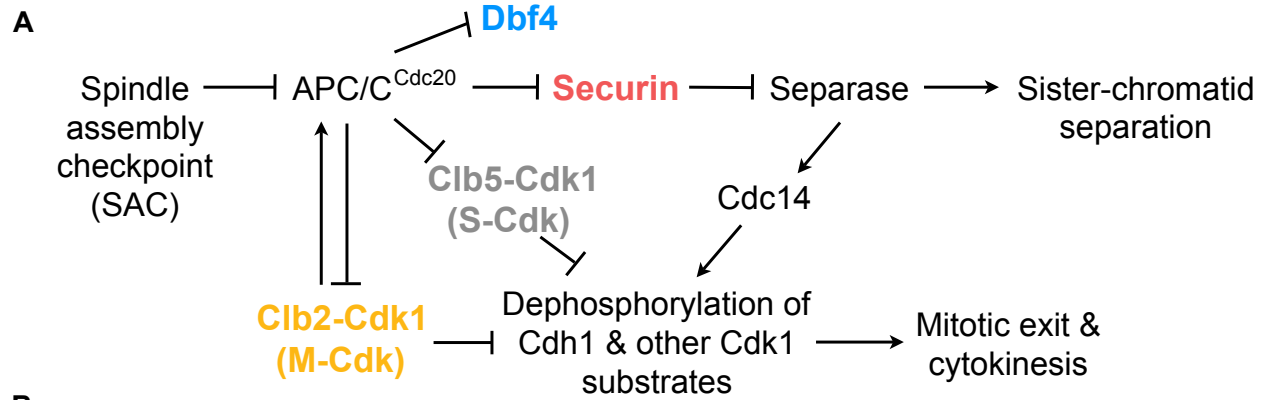


Figure 1. Metaphase-anaphase transition in cells carrying GFP-tagged APC/C substrates.

(A) Network diagram of the metaphase-anaphase transition in budding yeast. (B) GFP-tagged APC/C^{Cdc20} substrates and mCherry-tagged SPBs in cycling cells, at 3-min intervals. Dashed circles indicate cells at the onset of SPB separation, and solid circles mark cells at the onset of spindle elongation.

Figure 2

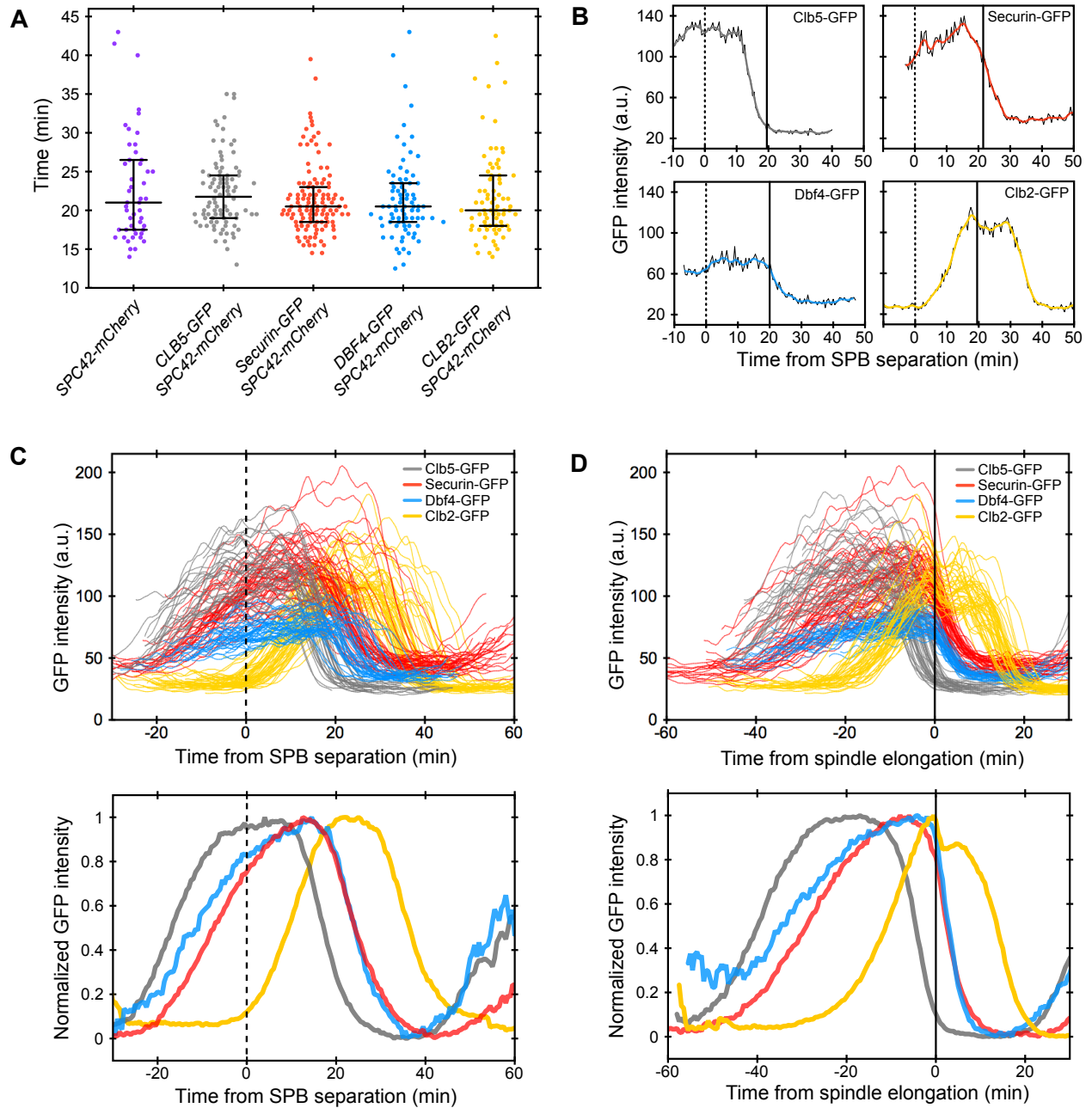


Figure 2. Timing and dynamics of APC/C^{Cdc20} substrate degradation. (A) Time from SPB separation to spindle elongation in individual cells with GFP tags on APC/C substrates. Each dot represents a single cell. Starting from left, sample sizes are: n = 49, 90, 121, 82, 77 cells. For each strain, the middle bar indicates the median value and error bars indicate the 25th and 75th percentiles. (B) GFP intensity of representative individual cells with tagged APC/C^{Cdc20} substrates (from the cell populations analyzed in A). Underlying black lines show the original data, and the colored lines are smoothed traces. The timing of SPB separation and spindle elongation are marked with dashed and solid lines, respectively. (C, D) Comparison of different GFP-tagged substrates using SPB separation (C, dashed lines) or spindle elongation (D, solid lines) as the timing reference (from the cell populations analyzed in A). In top panels, each line is a smoothed trace of a single cell. A random subset of representative cells is shown for clarity of viewing. Bottom panels show the averaged traces, where unsmoothed traces from all cells were first aligned to the same time reference point, averaged at each time point and then normalized to maximum intensity.

Figure 3

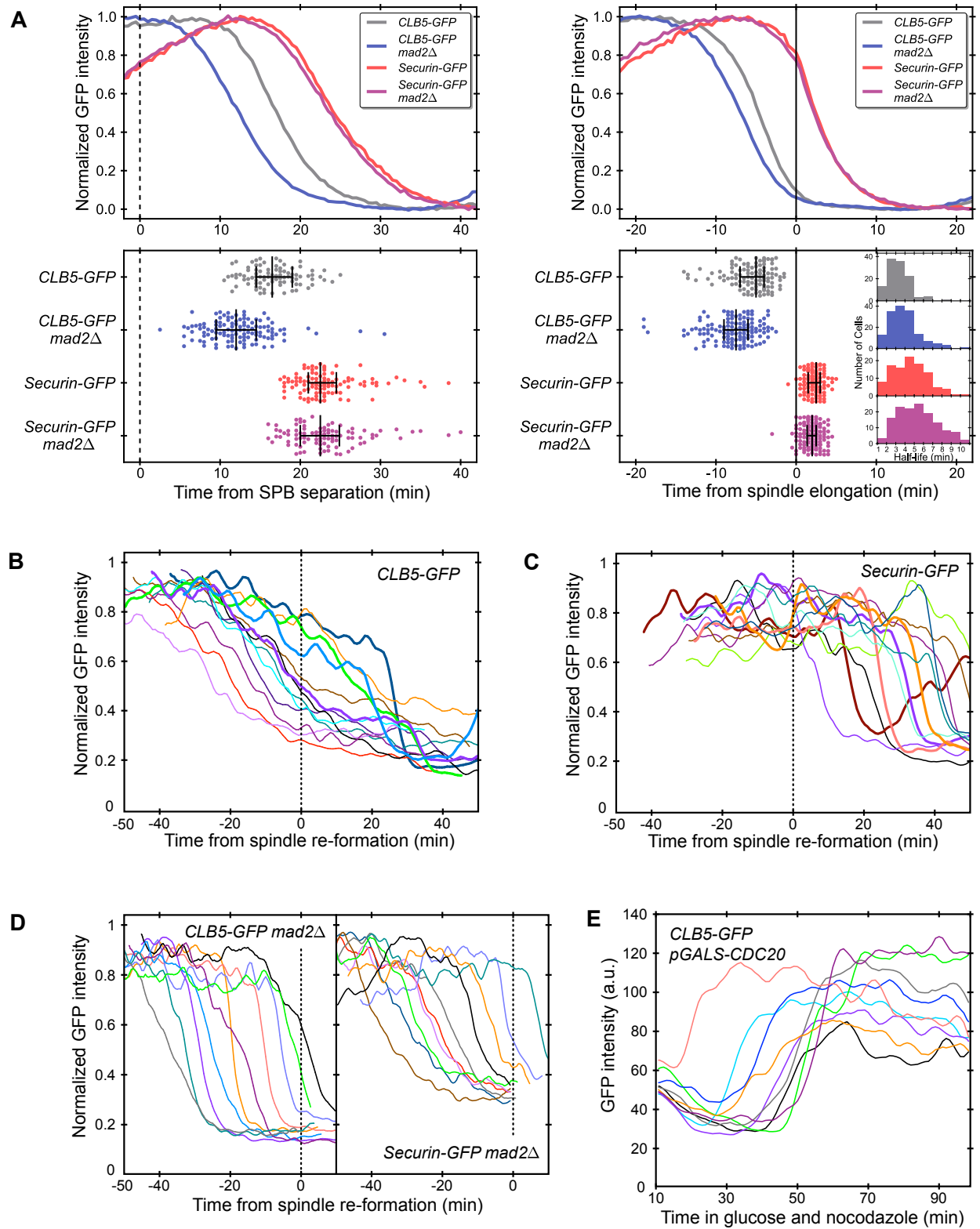


Figure 3. Role of the SAC in APC/C^{Cdc20} substrate degradation. (A) Clb5 and securin degradation profiles in wild-type and *mad2Δ* cells. Cells are aligned using either SPB separation (left panel, dashed line), or spindle elongation (right panel, solid line). Top panels show averaged and normalized traces as in Fig. 2C, D. Bottom panels show the time of 50% substrate degradation in individual cells (Fig. 8C). Each dot represents a single cell, and $n > 90$ cells per strain. For each strain, the middle bar indicates the median value, and error bars indicate the 25th and 75th percentiles. The insert in the lower right panel shows a histogram of rates of degradation in different strains, calculated from single cell traces; $n > 100$ cells per strain. (B, C, D) Clb5 and securin degradation in nocodazole-treated cells; $n > 20$ cells per strain. Asynchronous cells were plated on agarose pads with 15 $\mu\text{g/ml}$ nocodazole 10 min before imaging began. Representative traces from individual cells are normalized and aligned to spindle reformation (dotted line). The traces shown here were selected on the basis of two criteria: minimum overlap among traces for clarity of viewing, and inclusion of only mitotic cells, as judged by bud size. Wild-type (B, C) and *mad2Δ* cells (D) are shown. In (B, C), representative cells with fast substrate degradation after recovery from the SAC arrest are shown in bold lines. (E) Clb5 degradation in nocodazole with *CDC20* shut off; $n > 20$ cells. Asynchronous cells were grown in 2% galactose and plated on an agarose pad with 2% glucose and 15 $\mu\text{g/ml}$ nocodazole. Representative traces began 10 min after cells were plated on the agarose pad and were selected randomly.

Figure 4

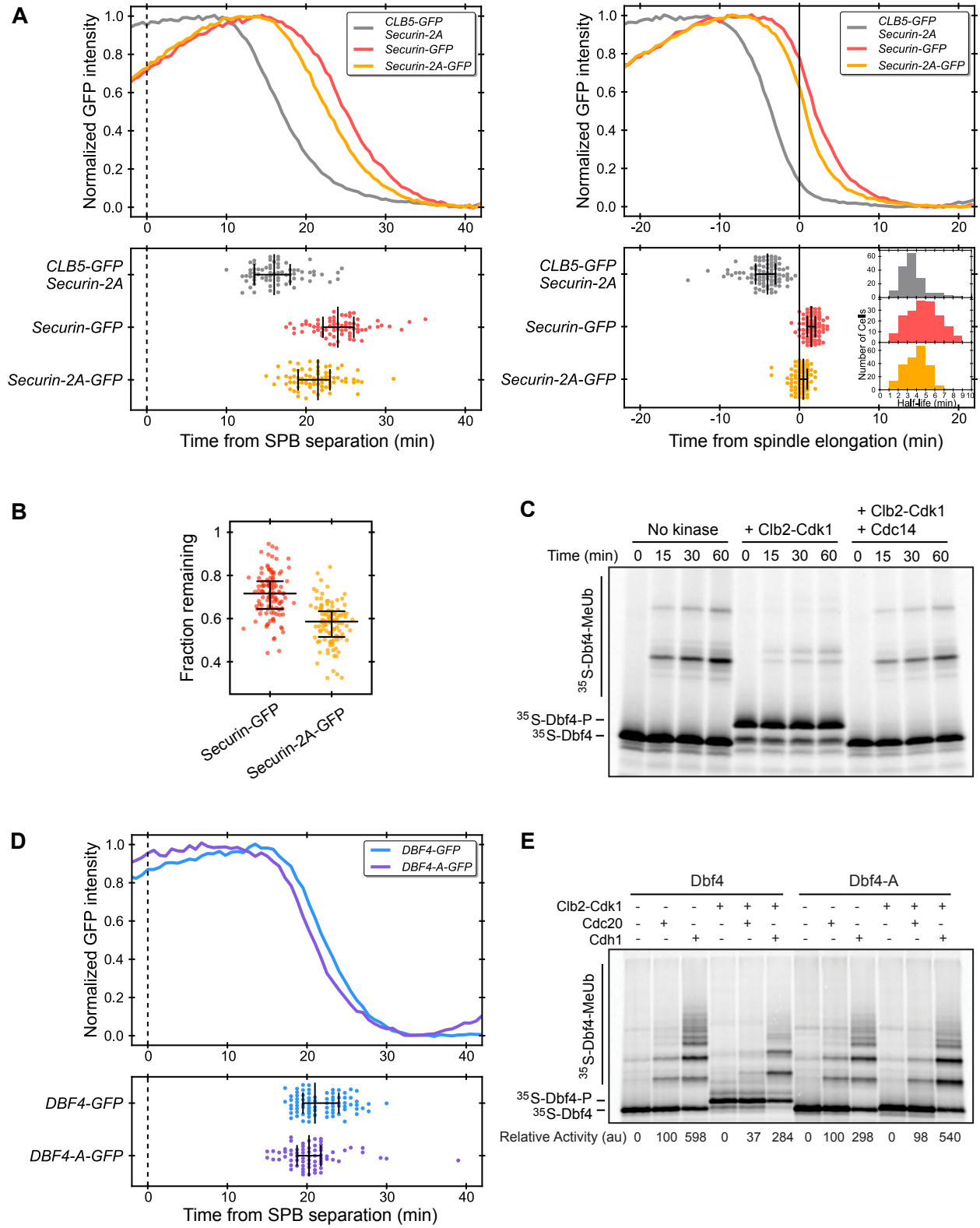


Figure 4. Role of phosphorylation by Cdk1 in APC/C^{Cdc20} substrate degradation. (A)

Degradation profiles of GFP-tagged securin-2A, wild-type securin and Clb5, as in Fig. 3A; n > 70 cells per strain, and in the insert, n > 160 cells per strain. (B) Fraction of securin or securin-2A remaining when spindle elongation occurs. Single-cell traces of GFP were smoothed, and the fraction remaining was calculated as the GFP intensity at spindle elongation divided by maximum GFP intensity. Each dot represents a single cell (n > 100 cells per strain). For each strain, the middle bar indicates the median value and error bars indicate the 25th and 75th percentiles. (C) Dbf4 ubiquitination by APC/C^{Cdc20} *in vitro*. Radiolabeled Dbf4 N-terminal fragment (residues 1-236) was produced by *in vitro* translation and incubated with buffer, purified Clb2-Cdk1, or both Clb2-Cdk1 and Cdc14, prior to the addition of purified APC/C, Cdc20, and other ubiquitination components for the indicated times. Reaction products were separated by SDS-PAGE and analyzed by autoradiography. (D) Dbf4 and Dbf4-A ubiquitination by APC/C^{Cdc20} or APC/C^{Cdh1} *in vitro*, as in panel C. (E) Degradation profiles of Dbf4-A-GFP and wild-type Dbf4-GFP, as in Fig. 3A; n > 70 cells per strain.

Figure 5

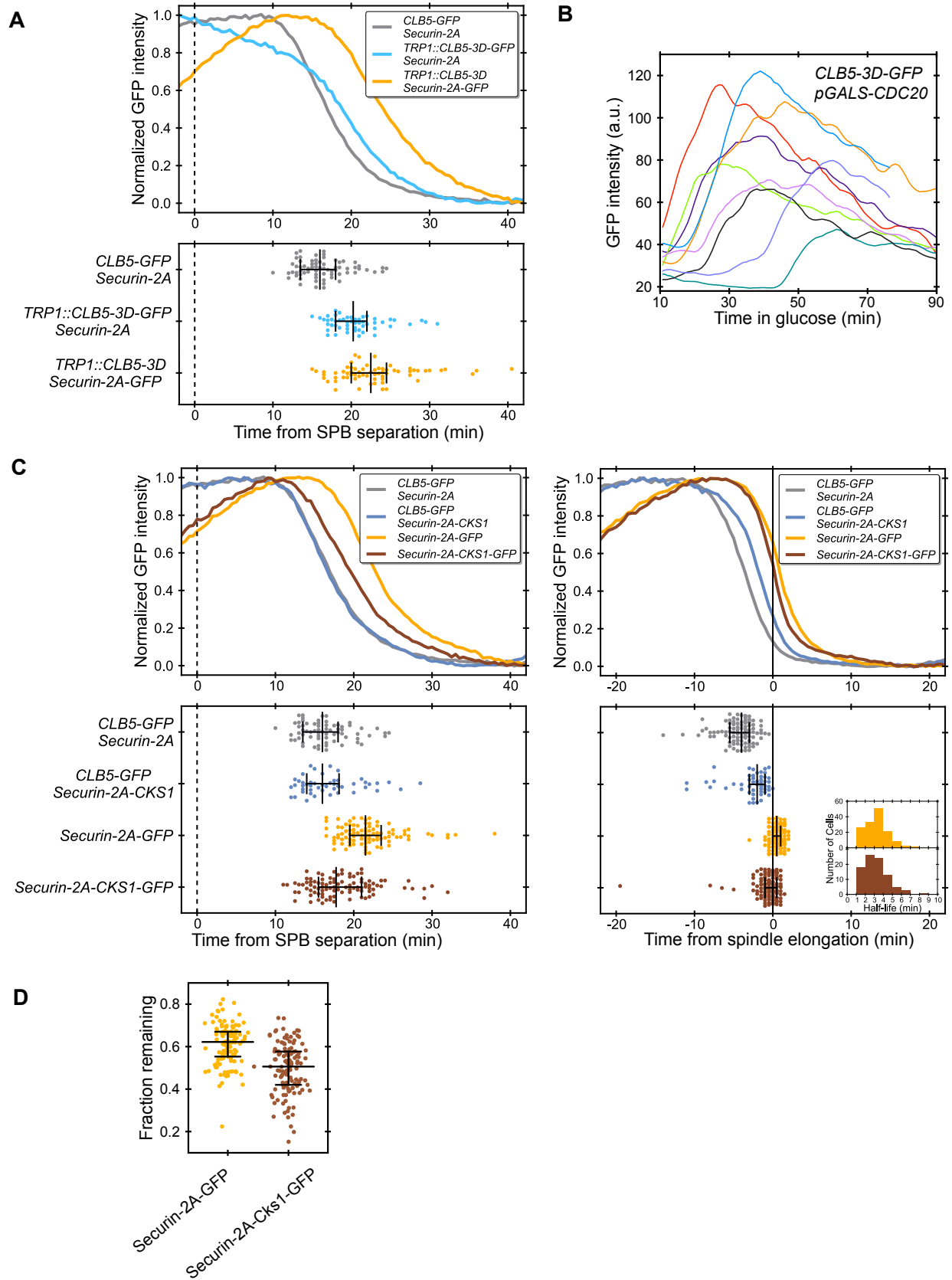


Figure 5. Contribution of Cdk1-Cks1 to Clb5 early degradation. (A) Binding of Cdk1 by Clb5-GFP, Clb5-2D-GFP (I166D, F291D) and Clb5-3D-GFP (F169D, F254D, F291D). Lysates of cells expressing wild-type or mutant Clb5-GFP from the endogenous *CLB5* promoter were incubated with GFP-binding protein coupled to sepharose beads. After washing, associated proteins were analyzed by SDS-PAGE and western blotting with anti-GFP and anti-Cdk1 antibodies simultaneously. (B) Degradation profiles of wild-type Clb5-GFP, Clb5-3D-GFP, and Clb5-3D-GFP-Cks1, as in Fig. 3A; $n > 70$ cells per strain. (C) Degradation profiles of securin-2A-Cks1-GFP, securin-2A-GFP, and Clb5-GFP in the securin-2A-Cks1 or securin-2A background, as in Fig. 3A; $n > 50$ cells in the Clb5-GFP strains and $n > 90$ cells in the securin-GFP strains. In the insert, $n > 100$ cells per strain. (D) Fraction of securin-2A or securin-2A-Cks1 remaining when spindle elongation occurs, as in Fig. 4B; $n > 100$ cells per strain.

Figure 6

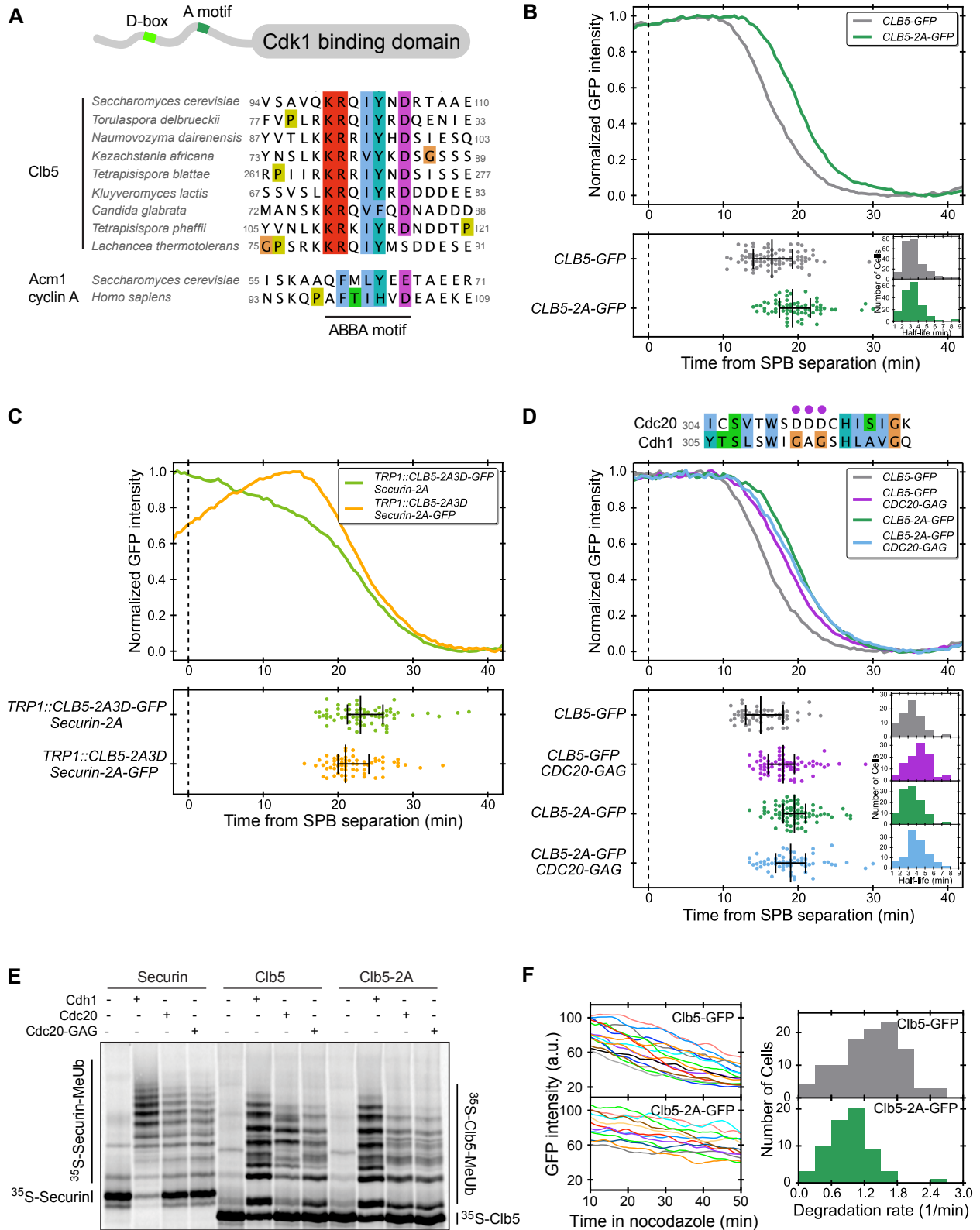


Figure 6. Contribution of the ‘ABBA motif’ to Clb5 degradation. (A) Sequence alignment of Clb5 orthologs from members of the yeast *Saccharomyces* clan, showing the putative ABBA motif in Clb5 in alignment with other known ABBA motifs. Different colors represent chemical properties of the residues. (B) Degradation profiles of Clb5-2A-GFP and wild-type Clb5-GFP, as in Fig. 3A; $n > 70$ cells per strain. In the insert, $n > 170$ cells per strain. (C) Degradation profiles of Clb5-2A3D-GFP and securin-2A-GFP, as in Fig. 3A; $n > 60$ cells per strain. (D) Sequence alignment of budding yeast Cdc20 and Cdh1; purple dots mark the potential ABBA motif-interacting residues that are different between Cdc20 and Cdh1. Below is the degradation profile of Clb5-2A-GFP or wild-type Clb5-GFP in a *CDC20-GAG* background, compared to the wild-type *CDC20* background; $n > 57$ cells per strain. In the insert, $n > 75$ cells per strain. (E) Analysis of Clb5 and Clb5-2A ubiquitination by APC/C^{Cdc20} or APC/C^{Cdc20-GAG} *in vitro*, as described in Materials and methods. Reactions with securin were included as controls. (F) Degradation of Clb5-GFP and Clb5-2A-GFP in nocodazole-treated cells. Asynchronous cells were plated on an agarose pad with 15 ug/ml nocodazole 10 min prior to the start of imaging. Clb5-GFP dynamics before spindle reformation (SAC inactivation) were analyzed. Representative traces were selected to minimize overlap and omit cells that were not in mitosis. Right panel shows the rates of degradation calculated by fitting single-cell GFP traces to a linear decay; $n > 55$ cells per strain.

Figure 7

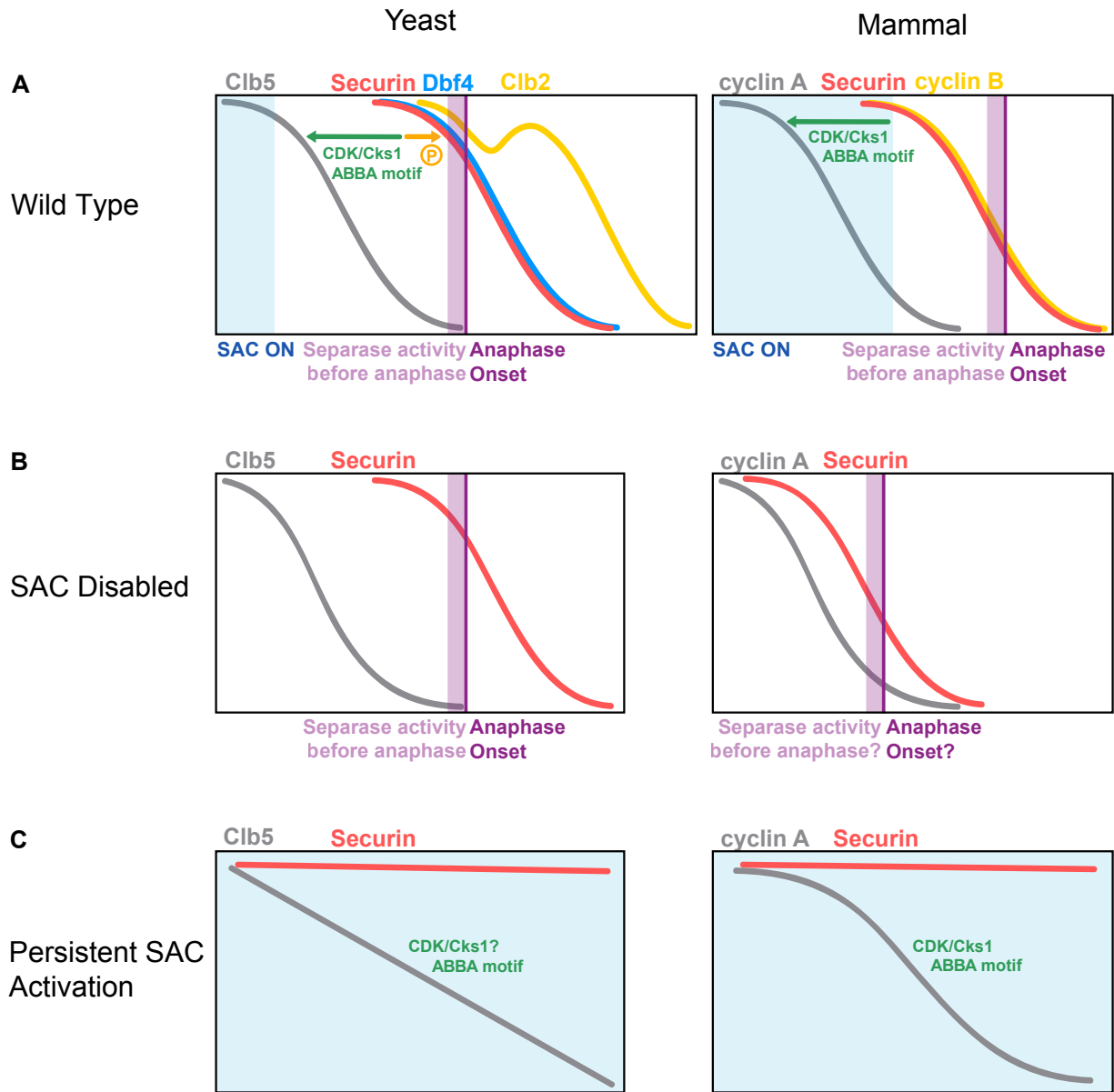


Figure 7. APC/C substrate degradation timing in yeast and mammalian cells. (A) Summary of the regulatory events leading to the metaphase-anaphase transition in yeast and mammalian cells, and the mechanisms that determine the timing and order of APC/C^{Cdc20} substrate degradation in wild-type cells. (B) In yeast, defects in SAC function cause earlier Clb5 destruction but do not affect the timing of securin destruction; in contrast, in mammalian cells SAC defects result in earlier cyclin A and securin destruction, and anaphase onset. (C) In a prolonged SAC arrest, securin is stable, whereas Cks1 and the ABBA motif promote slow degradation of Clb5 and cyclin A. The diagrams in this figure are based on the current work and many previous studies (Clute and Pines, 1999; Collin et al., 2013; den Elzen and Pines, 2001; Dick and Gerlich, 2013; Di Fiore, Davey, and Pines, submitted for publication; Di Fiore and Pines, 2010; Geley et al., 2001; Hagting et al., 2002; Shindo et al., 2012; Wolthuis et al., 2008; Yaakov et al., 2012).

Figure 8

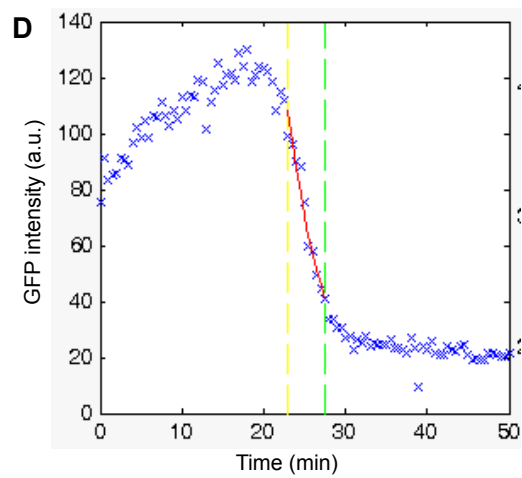
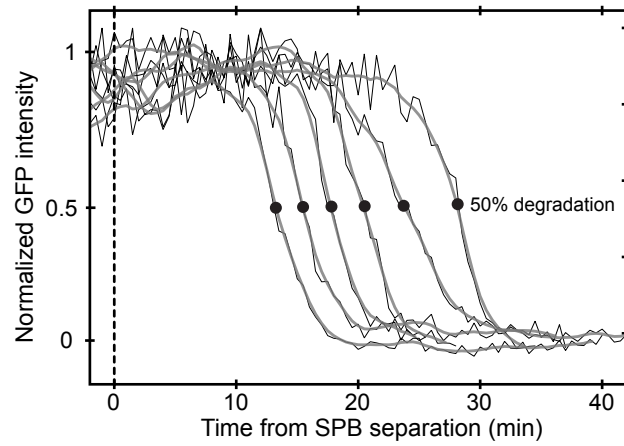
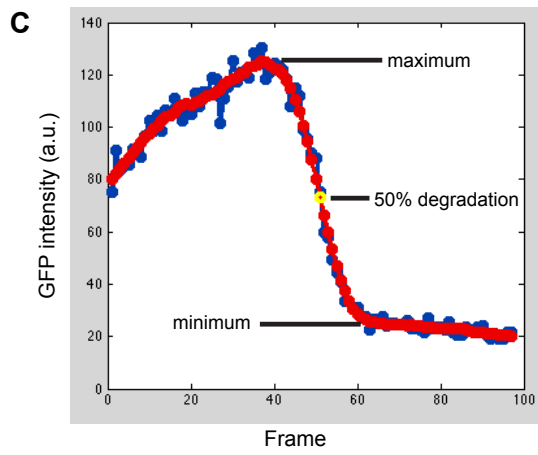
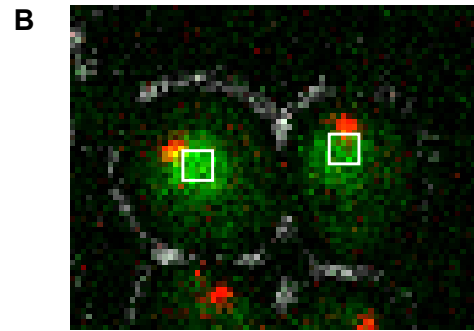
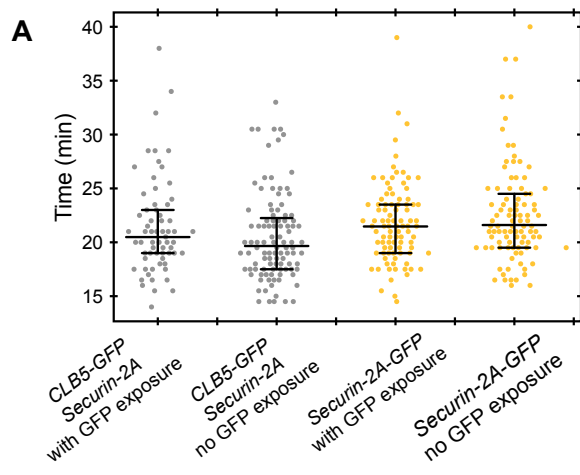


Figure 8. **Control experiment and data processing methods.** (A) Time from SPB separation to spindle elongation in individual cells with or without GFP exposure. The same strains were imaged with the mCherry channel alone or with both mCherry and GFP channels, to assess the impact on cell growth from imaging the GFP channel, which has higher energy than the mCherry channel. Each dot represents a single cell; $n > 65$ cells per strain. The middle bar indicates the median value, and error bars indicate the 25th and 75th percentiles. Student's *t*-test *p*-value = 0.18 and 0.21 for Clb5-GFP and securin-2A-GFP strains, respectively. (B) Quantification of GFP substrate signals within a square of 5x5 pixels, as described in Materials and methods. (C) Determination of the time point of 50% substrate degradation, as described in Materials and methods. Left panel: snapshot of the MATLAB program defining the midpoint of degradation (yellow circle). Blue trace shows the original data, and red trace shows the smoothed data. Right panel: black traces show the original data, and grey traces show the smoothed data. The black dots mark the midpoint of degradation, and correspond to the data points shown in the bottom panels of Fig. 3A. (D) Fitting of the degradation rate to a single exponential decay (see Materials and methods).

Figure 9

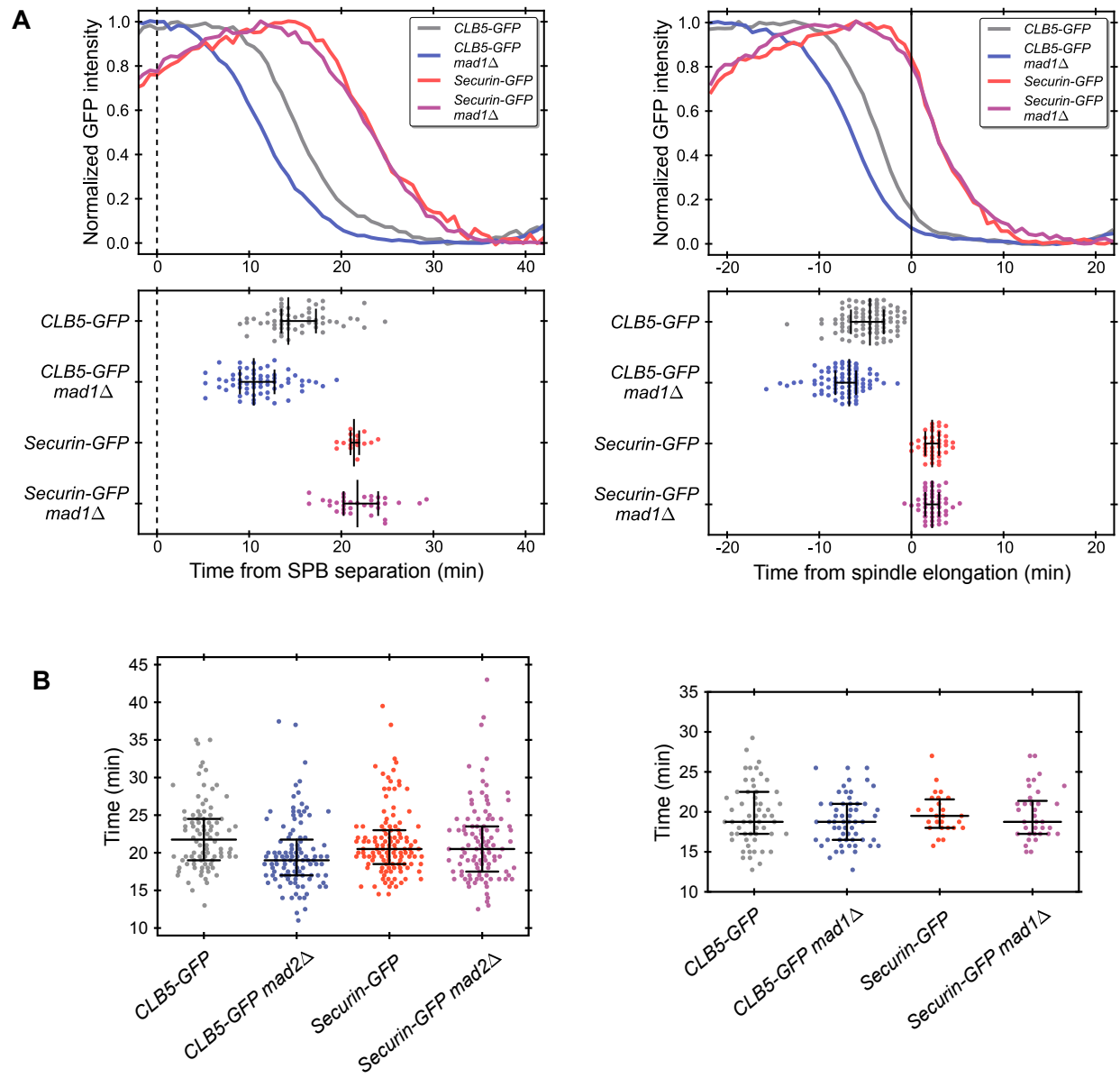


Figure 9. **Role of SAC in APC/C^{Cdc20} substrate degradation.** (A) Clb5 and securin degradation profiles in wild-type or *mad1*Δ cells, as in Fig. 3A. In bottom panels, n > 55 cells per Clb5-GFP strain, n > 16 cells per securin-GFP strain. (B) Time from SPB separation to spindle elongation in individual cells in SAC-disabled strains, as in Fig. S1A. Left panel, n > 90 cells per strain, one-way ANOVA *p*-value = 0.01; right panel, n > 26 cells per strain, *p*-value = 0.57.

Figure 10

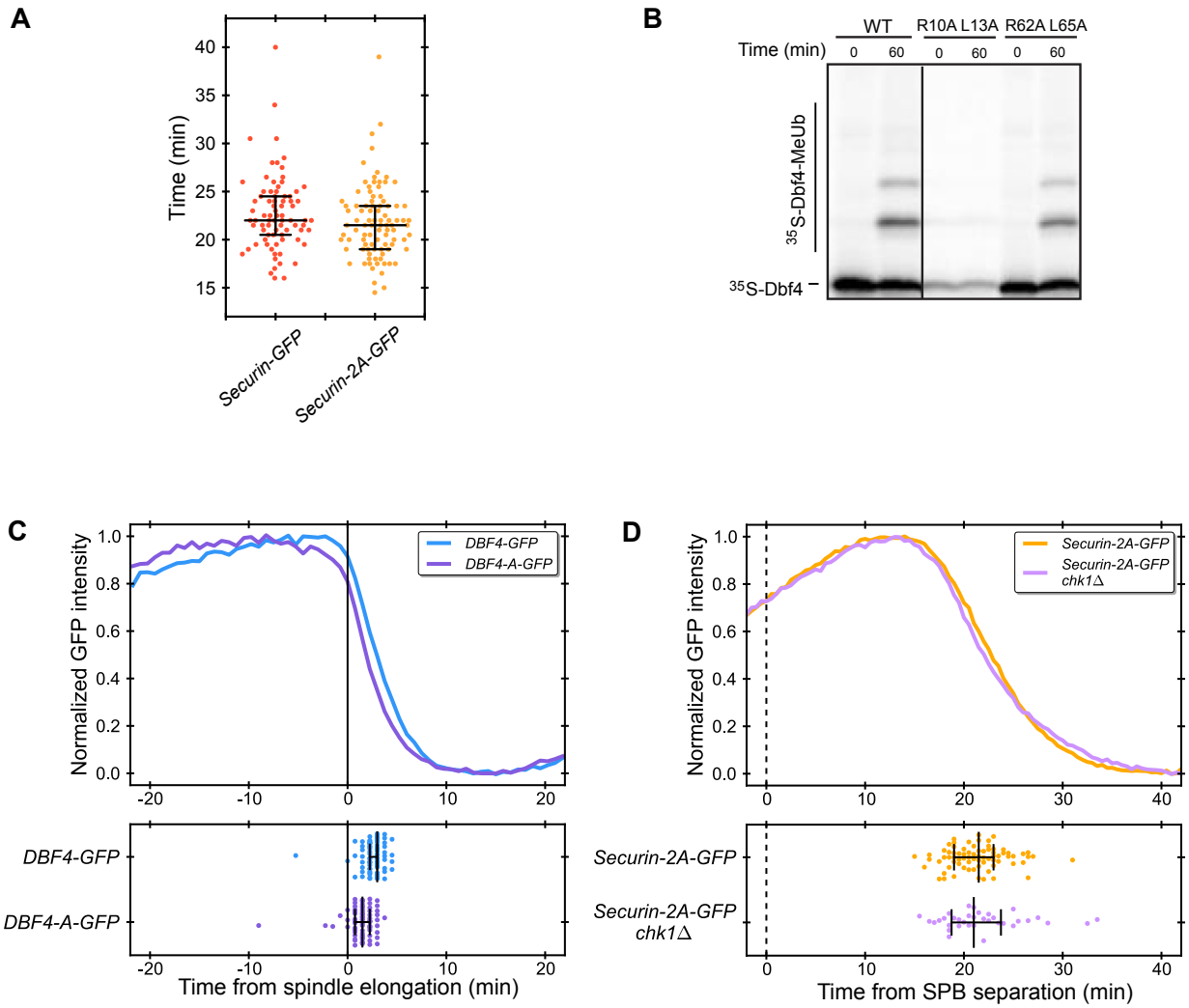


Figure 10. Role of phosphorylation in APC/C^{Cdc20} substrate degradation. (A) Time from SPB separation to spindle elongation in individual cells in the indicated strains, as in Fig. 8A; n > 30 cells per strain, *p*-value = 0.11. (B) Ubiquitination of wild-type and D-box mutant Dbf4 N-terminal fragment (236 residues) by APC/C^{Cdc20} *in vitro*. (C) Degradation profiles of Dbf4-A or wild-type Dbf4, as in Fig. 3A; n > 80 cells per strain, *p*-value < 0.001. (D) Degradation profiles of securin-2A in wild-type or *chk1*Δ cells, as in Fig. 3A; n > 50 cells per strain, *p*-value = 0.85.

Figure 11

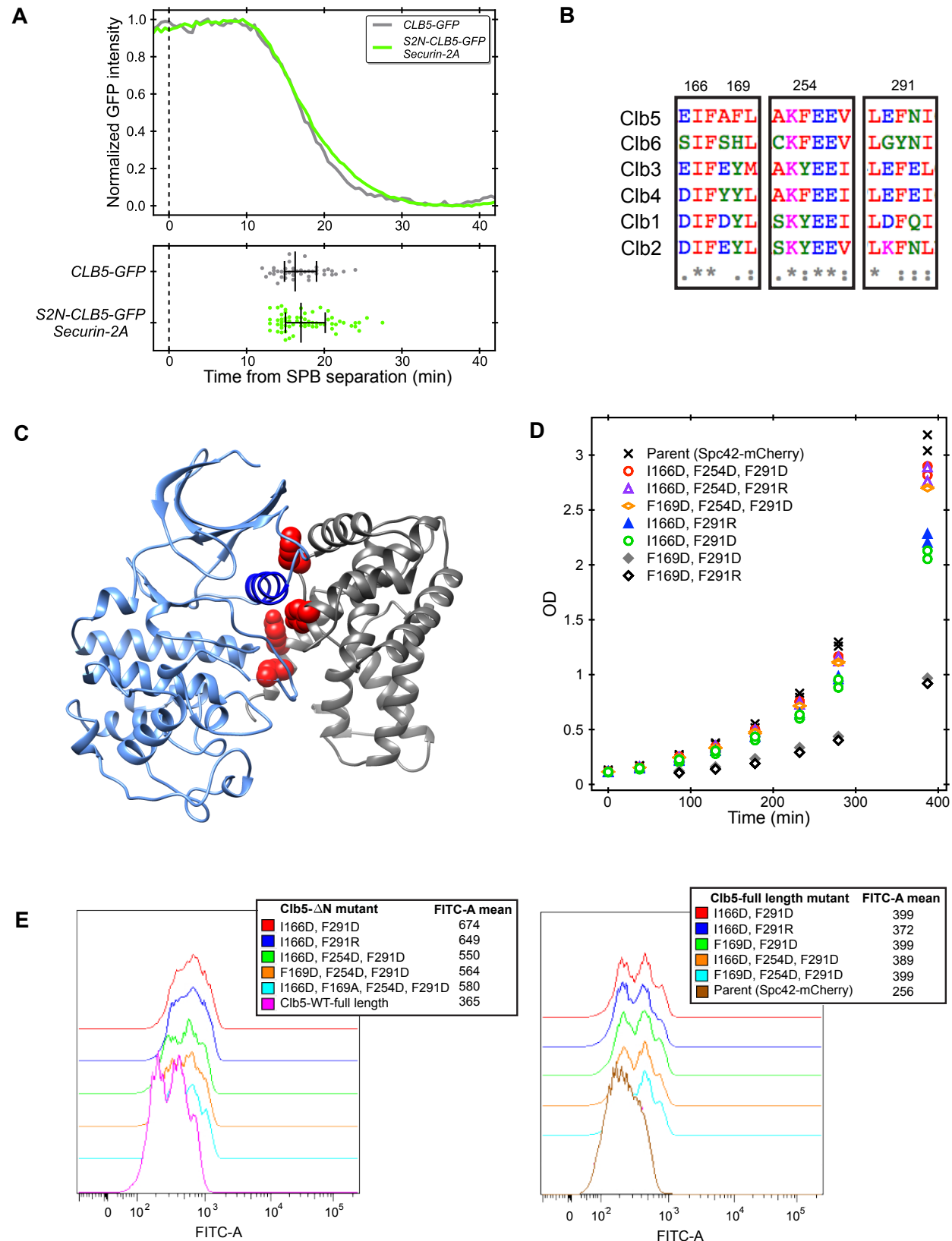
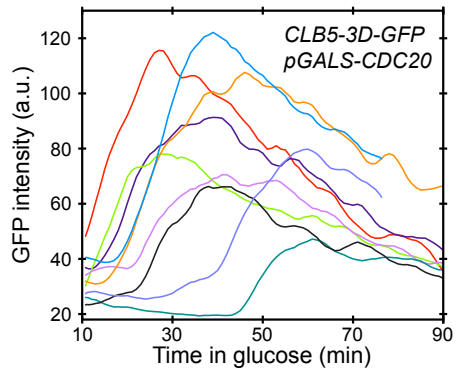


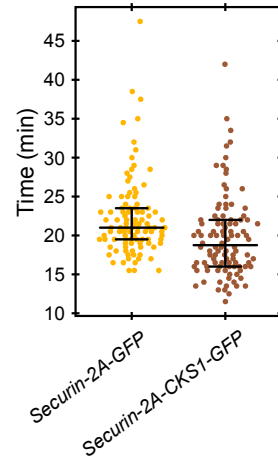
Figure 11. **Design of Clb5 mutants with decreased binding to Cdk1.** (A) Degradation profiles of wild-type Clb5-GFP and the S2N-Clb5-GFP chimera, in which the 95 N-terminal residues of Clb5 have been replaced with the 110 N-terminal residues of securin-2A. Presented in the same format as in Fig. 3A; $n > 40$ cells per strain, p -value = 0.23. (B) Sequence alignment of budding yeast B-type cyclins, with residue numbers at top indicating the four candidate residues at the Clb5-Cdk1 interface. Different colors represent chemical properties of the residues, and the symbols in gray indicate conservation. (C) Homology structure of the Clb5-Cdk1 complex based on the crystal structure of Cyclin B-Cdk2 (2jgz). Cdk1 is shown in blue, and the alpha helix involved in cyclin binding is highlighted in dark blue. Clb5 is shown in gray and the side chains of the candidate residues are shown in red. (D) Growth curves of cells expressing Clb5- Δ N with the indicated point mutations at candidate Cdk-binding residues. (E) Protein levels of Clb5- Δ N-GFP (left panel) or Clb5-GFP (right panel) bearing the indicated mutations expressed under the control of the *CLB5* promoter, as measured by flow cytometry.

Figure 12

A



B



C

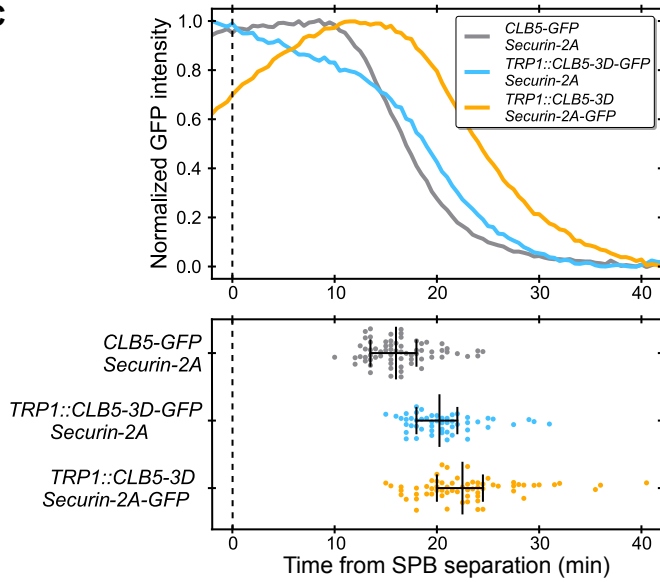


Figure 12. **Role of Cks1 in APC/C^{Cdc20} substrate degradation.** (A) Clb5-3D-GFP degradation following *CDC20* shutoff, as in Fig. 3E. (B) Time from SPB separation to spindle elongation in individual cells in the indicated strains, as in Fig. 8A; n > 100 cells per strain. (C) Degradation profiles of wild-type Clb5-GFP, Clb5-3D-GFP, and securin-2A-GFP, as in Fig. 3A; n > 50 cells per strain.

CHAPTER 3.

DYNAMIC SIMULATION OF

SUBSTRATE DEGRADATION

Introduction

APC/C is a multi-subunit RING-domain E3 ubiquitin ligase. It acts as a platform that bridges a substrate and an E2 charged with a ubiquitin to promote the ubiquitin transfer from the E2 to the substrate (Matyskiela et al., 2009). It is known for a long time that its activators Cdc20 and Cdh1, together with another subunit Apc10, provides substrate recognition for APC/C (Visintin et al., 1997; Schwab et al., 1997; Sigrist and Lehner, 1997; Fang et al., 1998; Kramer et al., 1998; Carroll et al., 2005). It is shown only recently that the binding of activators also induces a conformational change of APC/C core that facilitates the ubiquitin transfer (Chang et al., 2014; Van Voorhis and Morgan, 2014). A ubiquitin can be added to many lysine residues on the substrate surface, or it can be added to existing ubiquitins that is already attached to the substrate to build a ubiquitin chain. When one of these chains becomes longer than four ubiquitins, it can be recognized and degraded by the proteasome (Glickman and Ciechanover, 2002).

One remaining mystery from our previous results is that how those different mechanisms that regulate substrates degradation translate into distinct timing of substrate degradation. How do these different mechanisms modulate APC/C-substrate interaction? If they make one substrate better than another, how do they change the timing of degradation onset on top of the rate of degradation? In other words, why don't the later substrates start to degrade as soon as APC/C becomes active as indicated by Clb5 degradation?

We first analyzed the previous data and showed that the differences in degradation onset accounts for a major part of the overall differences in the degradation timing. Using a combination of experimental and computational approaches, we provided evidence that competition among substrates does not contribute significantly to the delay of later substrates.

Instead, for a single substrate, having a multi-step ubiquitination process can robustly produce a delay in substrate degradation while maintaining a fast degradation rate as observed. The delay and rate of degradation can be easily modulated by the interaction between the substrate and APC/C to generate different degradation profile. We last showed that in a system with two substrates and limited amount of APC/C, it is possible that the two substrates do not significantly influence each other.

Results

Substrate-APC/C^{Cdc20} interactions change the onset of substrate degradation

In our previous work, we estimated the timing of substrate degradation in single cells using when 50% of the substrate was degraded. It was a combinatorial indication of the timing of degradation onset and the rate of degradation. Here we directly measured the timing of degradation onset. For a single-cell GFP trace, we first smoothed the curve and calculated the first derivative. The minimum of the first derivative corresponds to the fastest declining point on the GFP trace during substrate degradation. Starting from that point, we looked for an earlier time point where the first derivative was sufficiently close to 0 and that was our estimate of degradation onset.

We quantified the timing of degradation onset for all of the strains in our previous experiments. We showed that mechanisms that regulate substrate degradation, such as securin phosphorylation, Cdk1 binding and ABBA motif of Clb5, all change the onset of the degradation significantly. In fact, delayed degradation onset is the major component of the overall delay in their degradation. (Fig. 13, comparing to previous figures).

Competition among substrates is not responsible for the timing difference

The differences in degradation onset among the substrates can potentially be explained by their competition for active APC/C^{Cdc20}. In this case, APC/C is in limited quantity and is first occupied by better substrates such as Clb5 and only becomes available for other substrates when the majority of Clb5 is degraded. If this were true, removing the best known substrate Clb5 should allow later substrates to be degraded earlier, and adding extra Clb5 to the cell should delay the degradation of later substrates. Deletion of Clb5 causes DNA replication defects and slow down cell growth dramatically and could complicate our measurement of mitotic timing (Schwob and Nasmyth, 1993). In our previous experiments we replaced the endogenous Clb5 with the Clb5-2A mutant, where its Cdc20-interacting ABBA motif is mutated. This resembles a Clb5 deletion scenario. The Clb5-2A mutant is a much less-efficient substrate for APC/C, and if the delay in its degradation is dependent on better APC/C substrates such as Clb5, without Clb5, Clb5-2A should degrade as soon as APC/C^{Cdc20} becomes active when normally Clb5 degradation starts. However, the onset of Clb5-2A degradation is still much later comparing to wild-type Clb5 (Fig. 13E). Furthermore, we introduced an extra copy of Clb5 driven by its own promoter into cells with the securin-2A allele. These cells maintain their endogenous copy of Clb5, while securin is replaced by securin-2A, whose degradation is not regulated by Cdk1 phosphorylation and directly drives anaphase onset. The extra copy of Clb5 was tagged with GFP to confirm its expression in the cell. Adding the extra Clb5 did not have any dramatic effect on the time duration from SPB separation to spindle elongation (Fig. 13F), the latter of which is strongly correlated with securin degradation. With these evidence, we believe that competition among substrates does not play a major role in determining the timing of substrate degradation.

A simple dynamic model for APC/C ubiquitination

It seemed to us that delayed substrate degradation relative to APC/C^{Cdc20} activation, such as in the case of Clb5-2A and securin-2A, does not rely on the existence of other competing substrates. Given the fact that Clb5-2A has only two amino acid difference comparing to wild-type Clb5, and these two mutations are known to specifically disrupt interaction with Cdc20, it is highly unlikely that they differ in their interaction with other protein players that we did not take into account. We thus wondered whether it is possible to generate a robust delay in substrate degradation simply relying the interaction between one substrate and APC/C^{Cdc20}.

To address this question, we developed a dynamic model (Fig. 14A). The model has one type of substrate S that can bind to and get ubiquitinated by APC/C. It is comprised of the following molecular species: free APC/C (A); free un-modified substrate (S0), free substrate with one, two, three or four ubiquitin attached (S1, S2, S3, S4 respectively); APC/C-bound un-modified substrate (AS0), and APC/C-bound substrate with one, two, three or four ubiquitin attached (AS1, AS2, AS3, AS4 respectively). These molecular species interact and interconvert according to the following rate constants: APC/C and free substrates associate with rate constant k_a ; APC/C-bound substrates can either dissociate with rate constant k_d or get one more ubiquitin attached with rate constant k_c ; once a substrate has four ubiquitins, regardless of whether it is bound to APC/C, it will be degraded with rate constant e ; APC/C is activated linearly at rate p_a starting from time 0, and we assumed no production of substrates as protein levels of Clb5 and Clb5-2A plateau for several minutes before their degradation begins. The concentration change of each molecular species was determined by ordinary differential equations and all reactions were modeled as mass action since we considered binding and catalysis steps explicitly.

The initial concentration of the substrate is 200nM, estimated by the protein concentration in the yeast nucleus (Ghaemmaghami et al., 2003). The rate of APC/C activation p_a is 0.06nM/s, so that it becomes comparable to the concentration of substrate in the end of simulation (Ghaemmaghami et al., 2003). The degradation rate constant e is fixed at 1000/s, so that as soon as a substrate gets four ubiquitins it will be degraded. When we scanned the parameters, to cover the whole physiologically-relevant range, we varies k_c and k_d from $10^{-3}/s$ to $10^3/s$ as estimated by *in vitro* enzymatic reaction results (Carroll et al., 2005; Van Voorhis and Morgan, 2014). Association rate constant k_a , assumed to be diffusion-limited, ranges from $10^4/nM/s$ to $10/nM/s$. For each parameter in the range above, we took 25 sample points for k_c , k_d , and 21 sample points for k_a evenly distributed on a log scale, so that each parameter value changes by 1.8 fold comparing to its immediate neighbors. Then for each set of parameter, we calculated the dynamics of the substrate concentration over a time period that resembles the duration of a movie for experimental analysis (Fig. 14B).

Delay in degradation onset and fast degradation rate are opposing constraints

For each set of parameters, to quantify the delay on degradation onset, we measured the time duration from time 0s when APC/C activity starts to accumulate, to the time substrate concentration reaches 95% of initial value (T_{95}). To estimate the rate of substrate degradation, we measured the time duration from T_{95} to when 50% of substrate is degraded ($T_d = T_{50} - T_{95}$) (Fig. 15A). What became immediately obvious was that these two criteria: having a good delay in degradation onset ($T_{95} > 200s$), and a fast degradation ($T_d < 600s$, both estimated from experiment), favor distinct parameter regions. At any fixed association rate constant k_a , a good T_{95} requires small ubiquitination rate constant k_c , and/or big dissociation rate constant k_d ,

whereas a good T_d requires big k_c and/or small k_d (Fig. 15B). So in order to satisfy both, the working parameter region is restricted to a small area, and within this area, we can easily reproduce Clb5-2A degradation dynamics observed *in vivo* (Fig. 15C).

It is worth pointing out that when the dissociation rate constant k_d is 0/s, the substrate binds to APC/C and obtains four ubiquitins before ever dissociating. In this case, the multi-step ubiquitination process resembles a single step enzymatic reaction, where the ubiquitination rate constant k_c determines both the timing of degradation onset, and the rate of degradation. As the dissociation rate constant k_d increases, substrates can dissociate from APC/C before they obtain four ubiquitins, and this results in accumulation of intermediate products. In this case, the degradation dynamics is a combined result of k_c and k_d as we will explore below.

Increasing association rate constant k_a changes the region of k_c - k_d that meets both T_{95} and T_d requirements. However the working region seems to always consist of two distinct sub-regions. In Region I, the value of k_c stays relatively constant, and in Region II k_c and k_d co-vary with a slope of 1 (Fig. 15D).

Deubiquitination is not necessary to create a robust delay

Balance between phosphorylation and dephosphorylation is thought to play an important role in ordered Cdk substrate dephosphorylation in late mitosis (Bouchoux and Uhlmann, 2011). We thus analyzed the role of deubiquitination in our model. We incorporated a deubiquitination rate constant k_{dub} into the model in different ways: 1) allowing deubiquitination for all substrates with ubiquitins attached, bound to APC/C or not; 2) allowing deubiquitination for only free substrates; 3) allowing deubiquitination for only APC/C-bound substrates; or 4) allowing deubiquitination for only substrates with one ubiquitin attached.

In all scenarios, including a deubiquitination reaction shrank the number of kc-kd combinations that produce a desired substrate degradation at a given ka. The bigger the kdub is, the less kc-kd combinations that work. It is because that kdub contributes to the delay of degradation onset but meanwhile negatively impact the degradation rate. Even though deubiquitination is likely to exist *in vivo*, it is not essential to reproduce experimental observations, and we thus excluded it from future analysis.

Varying dissociation rate constant kd only influences degradation timing in Region II

We next asked, given a set of parameters that can faithfully reproduce Clb5-2A degradation, whether it is possible to modify certain parameters to reproduce Clb5 degradation. *In vivo*, Clb5 may have a smaller dissociation rate constant kd than Clb5-2A due to the ABBA motif-Cdc20 interaction, or less intuitively, Clb5 may activates APC/C^{Cdc20} better than Clb5-2A through the ABBA motif and result in a bigger catalytic rate constant kc. The association rate constant ka is usually determined by random collision of molecules and is less likely to be different among substrates.

We first investigated the contribution of kc and kd to the delay in degradation onset. We fixed ka, and for each combination of kc-kd, we increased kc by 1.8-fold and measured the fold change of T95 as $(T95(kc)-T95(1.8*kc))/T95(kc)$. For each combination of kc-kd, we also decreased kd by 1.8-fold and calculated the fold change of T95 as $(T95(kd)-T95(kd/1.8))/T95(kd)$. In this case we analyzed the entire kc-kd space except those too slow to complete substrate degradation within the time window of simulation.

By comparing the influence of changing kc and kd, we learned a few things. First, increasing kc or decreasing kd both speed up the ubiquitination process and decreases T95 as

expected (Fig. 16A left and middle panels). Second, varying k_c has a significant impact on T95 in almost the entire parameter space, whereas varying k_d only has a significant impact in the area that overlap with Region II (Fig. 16A, B right panels). Third, in this region, starting from one combination of k_c - k_d , increasing k_c or decreasing k_d by the same fold leads to very similar change in T95 as indicated by the color. In other words, increasing k_c and meanwhile increasing k_d by the same fold would lead to almost no change (Fig. 16B). This results in the slope of 1 in Region II in Fig. 15D.

Varying dissociation rate constant k_d mainly influences degradation rate, not delay, in Region I

We also investigated the contribution of k_c and k_d to degradation rate. At a fixed k_a , we measured T_d for each combination of k_c - k_d . Like T95, T_d change monotonically with k_c . However, this is not the case with k_d . In a certain region, which we believe to overlap with Region I, as k_d increases, T_d first decreases and then start to increase (Fig. 16C top panels). To understand this, we examined the time course of substrate degradation. Starting from a small value, increasing k_d only slightly increases the delay. Instead, it dramatically increases the sharpness of the curve and thus leads to decreases in T_d . Only when k_d reaches a certain level, increasing k_d starts to significantly increase the delay and meanwhile slow down the degradation rate (Fig. 16C right panel). To confirm this result, we measured the slope at the time point where 50% of substrate remains as an estimate for the fastest degradation rate. Indeed, increasing k_d first leads to a steeper slope before it becomes more gradual (Fig. 16C bottom panels).

This observation has important implications. Depends on which parameter region the less efficient substrates, such as Clb5-2A and securin-2A, fall within, by simply improving binding

affinity to APC/C and thus decreasing k_d may not necessarily result in a degradation onset that is significantly earlier as observed for wild-type Clb5. Increasing the catalytic rate constant k_c on the other hand, could faithfully reproduce wild-type Clb5 degradation timing regardless of the parameter region.

Influence of the dissociation rate constant k_d is dependent on association rate constant k_a

We wondered what causes the differential influence of k_d on substrate degradation in distinct regions. The boundary of these regions varies with k_a in the same way as the boundary of Region I and II (Fig. 17A). Upon closer examination we discovered that with relatively small k_d , there is little free APC/C in the system before the majority of substrates are degraded. Only when k_d increases beyond a certain level, free APC/C starts to exist and changing k_d leads to a more significant change in T95 (Fig. 17B). This turning point varies with association rate constant k_a , because at a given substrate and APC/C concentration, k_a and k_d together determines the portion of free APC/C in the system.

This turning point separates the regions where k_d does not and does significantly influence T95. In the former region, T95 mostly rely on k_c and that leads to the Region I where k_c do not vary with k_d to produce a desired T95. In the latter region, varying k_d and k_c both significantly influence T95, and that leads to the co-variation slope of 1 as seen in Region II.

Competition among substrates is only prominent when there is a difference in binding affinity

So far we have been analyzing a system with only one substrate. To understand how competition could influence substrate degradation timing, we introduced a second substrate C

into the system. C interacts with APC/C the same way as S, and they now share and compete for the same pool of active APC/C. The only difference is that C is better than S in a similar way as Clb5 comparing to Clb5-2A or securin-2A, presumably by having a smaller dissociation rate constant k_d or a bigger catalytic rate constant k_c . And we aim to reproduce two experimental observations. First, Clb5 degrades earlier than Clb5-2A and securin-2A at a similar or slightly faster rate. Second, adding an extra copy of Clb5 would not significantly delay securin-2A degradation.

We compared the timing of S degradation onset in the following scenarios: (1) S is the only substrate in the system; (2) C starts in the same concentration as S, and k_d for C is 1/10 of k_d for S; (3) The concentration of C is twice the amount of S, and k_d for C is 1/10 of k_d for S; (4) C starts in the same concentration as S, and k_c for C is 10-fold of k_c for S; (5) The concentration of C is twice the amount of S, and k_c for C is 10-fold of k_c for S.

It became immediately clear that if C binds much tighter than S as in (2) or (3), in a large parameter region, the addition of C significantly delays the degradation of S comparing to (1) (Fig. 18A middle top and left panels). That is because in (2) and (3), C dominantly occupies the majority of APC/C and sequesters them away from S. Interestingly in this region, C seems to have a slower degradation rate comparing to S (Fig. 18A left panel). Indeed, the difference of T_{50} between C and S, is consistently smaller than the difference of T_{95} between C and S in this region (Fig. 18A middle bottom panel). This is similar to the effect of decreasing k_d in Region I in a one-substrate system, where it decreases the sharpness of degradation curve (See Fig. 16C). Thus this region does not agree with either of our experimental observations.

The region where C has little impact on S is where k_d is big enough to maintain a significant pool of free APC/C, and thus the competition between substrates become less

prominent (Fig. 18A right panel). In this region, C and S behave similarly to our experimental observations. The location of this region also varies with association rate constant k_a for the same reason as Region II in a one-substrate system (See Fig. 17).

On the other hand, if C is more efficient in acquiring ubiquitin once bound to APC/C as in (4) or (5), inclusion of C in the system has very minimal effect on the degradation of S in the entire parameter region (Fig. 18B). This is because that C binds APC/C equally well as S and they ‘friendly’ share the pool of available APC/C. Since the two substrates has little influence on each other, the delayed degradation of S is due to its interaction with APC/C as we examined in the one-substrate system. As for C, due to a faster k_c , it always degrade with a shorter delay and faster rate comparing to S regardless of the parameter region. This scenario also agrees with our experimental observations.

Discussion

There were three major experimental observations that was unexplained. First, different APC/C substrates start to degrade at different time and some of them don't start to degrade until APC/C has been active for several minutes. Second, with different timing of degradation onset, Clb5 is degraded at a similar or faster rate comparing to Clb5-2A and securin-2A. Third, early substrate Clb5 does not seem to be necessary or sufficient for delayed degradation of later substrates. From our modeling results, these can be explained by a system where substrates are relatively independent of each other, and their timing of degradation onset is determined by their interaction with APC/C. A substrate that takes longer to acquire enough ubiquitins for efficient degradation, either due to less tight binding to APC/C (bigger k_d) or slower catalytic rate once it is bound (smaller k_c), will take longer to initiate degradation. While k_c plays a big role in

determining both the delay in degradation onset and degradation rate, varying k_d can adjust the rate of degradation while maintaining a similar delay. Thus depending on region of parameters, varying these two parameters can easily reproduce the different degradation dynamics we observed among substrates.

Our one-substrate model resembles the situation where a substrate is not influenced by the other substrates, and it helped us understand how varying each parameter influences the degradation dynamics. Our two-substrate model is more similar to the real system and helped us understand in what scenario competition between substrates is prominent, and in what scenario substrates are more independent and can be approximated by the one-substrate model. If the two substrates have different k_c , our two-substrate model showed that they do not significantly influence the degradation of each other. Our one-substrate model then showed that in almost the entire parameter region, a bigger k_c would easily lead to an earlier degradation onset for the better substrate comparing to the other. If the two substrates have different k_d , on the other hand, the outcome would depend on parameter region. Based on the two-substrate model, if the balance between dissociation rate constant k_d and association rate constant k_a allows no free APC/C in the system, the better substrate would significantly delay the degradation of the other substrate and meanwhile degrade at a slower rate than the other substrate. This is in contrary to what we observe experimentally. If there is free APC/C in the system, the better substrate would not significantly impact the other substrate and would also degrade at a faster rate than the other one. Behavior in this region agrees with experimental observation, but it requires a k_d that is sufficiently big depending on k_a and *in vivo* APC/C concentration.

It is not clear yet what the mechanisms that influence substrate degradation timing, such as securin phosphorylation, Cdk1 binding and ABBA motif of Clb5, actually do. Do they change

the binding affinity for APC/C, the catalytic rate, or something we did not consider in the model? It is easy to imagine how they can influence the substrate-APC/C binding affinity, as Clb5 have Cdk1-Cks1 and ABBA motif as extra APC/C binding sites. Indeed, it is shown in mammalian systems that the ABBA motif of cyclin A promotes better binding to Cdc20 (J. Pines, personal communication). It is also possible for them to change the catalytic rate. For example, Cks1 preferably bind phosphorylated APC/C, which are more active (Rudner and Murray, 2000); ABBA motif might help substrate to orient Cdc20 to better activate APC/C. It is important to point out that these possibilities are not mutually exclusive, and in fact a combination of increased binding affinity and catalytic rate would additively aggravate the differences among substrates. Future experiment is needed for a more complete understanding of the system.

Similar to APC/C, ordered substrate phosphorylation by Cdk1 is an essential feature of cell cycle regulation. It was shown that it is dependent on different specificity (estimated by k_{cat}/K_m , K_m is the Michaelis–Menten constant) for substrates (Kõivomägi et al., 2011). The sequential dephosphorylation of Cdk1 substrates were also shown to be a combinatorial result of Cdk1 specificity and the phosphatase Cdc14 specificity (Bouchoux and Uhlmann, 2011). Here for APC/C substrates, we broke down the specificity to its components: catalytic rate, association rate and dissociation rate, and showed that each of them contributes differently to the substrate degradation dynamic. Besides, we were able to not only measure the timing of substrate degradation but also the rate of degradation. We showed that a late onset of degradation and a fast degradation rate are stringent requirement for a system, as they prefer opposite trends of parameters. For this reason, having a reverse deubiquitination reaction in the system is not necessarily better. It helps establish a delay in substrate ubiquitination but meanwhile slows down the rate of degradation and thus could compromise a sharp transition. However in a

cellular context, having a low-level basal reverse reaction could be important to filter out fluctuation in APC/C activity before its activation and prevent unwanted substrate degradation.

One related distinction to make is the steady-state behavior of a system and its dynamical properties. Positive feedbacks contribute to the ‘sharpness’ of transitions by making the input-output relationship more ‘switch-like’. A ‘threshold’ is the input level below which there is little output, and above which there is significantly more output. They are both steady-state properties, meaning that the ‘output’ is defined by the steady-state level, and it says very little about dynamics. In the case of securin, Cdk1 phosphorylation inhibits its degradation, however its degradation promotes its dephosphorylation by activating Cdc14 downstream of separase. This establishes a positive feedback for securin degradation, yet the wild-type securin degrades slower than securin-2A which does not have the feedback. It is because the phosphorylation slows down its degradation rate. Another example is the contribution of deubiquitination to substrate degradation. This reverse reaction could establish a ‘threshold’ and allow an ‘all-or-none’ response. When APC/C^{Cdc20} activity is not enough to overcome the deubiquitination rate, there will be no substrate degradation, and only when APC/C^{Cdc20} activity goes above the ‘threshold’, there will be substrate degradation. However, having deubiquitination reaction unavoidably slows down the rate of ubiquitination and substrate degradation. Even though these concepts can be essential for decision-making processes, such as when analyzing the reversibility of transitions, it is important to be cautious relating them to the dynamical properties of the system.

Our model greatly simplified the process of ubiquitination by APC/C in several ways. First, the substrate usually has multiple accessible lysines for ubiquitin attachment. Instead of one chain, the substrate usually have several ubiquitin chains, and when one of them has more than four ubiquitins, the substrate is subject to proteasomal degradation (Glickman and

Ciechanover, 2002). Second, we did not explicitly consider E2 in our model and instead grouped it as part of APC/C. In budding yeast, the APC/C works with two E2s. Ubc4 is better at attaching ubiquitins to the lysines on the substrate and initiate attachment of ubiquitin chains. Ubc1 is better at attaching ubiquitins to other ubiquitins and extending the length of existing ubiquitin chains (Rodrigo-Brenni and Morgan, 2007). Thus they have different catalytic rate for different types of ubiquitin attachment, and the concentration of E2s could also matter. A related simplification is that we assumed equal rates for all steps of ubiquitination. Third, there are many different types of deubiquitinating enzymes in the cell, and the deubiquitination for APC/C substrates could occur in a more complex way than we considered, such as it strongly prefer short ubiquitin chains (Schaefer and Morgan, 2011). Fourth, we assumed no substrate production in the model based on the fact that Clb5 level plateaus before its degradation. For other substrates however, the production could contribute to their timing of degradation onset, as the ‘degradation onset’ we observe in experiment is in fact the moment when protein degradation overcomes the production. Last, the step of proteasomal degradation is not limiting in our model, based on the following observations. All the mutations we made specifically modulate substrate-APC/C interaction and they have an impact on substrate degradation. Besides, if the proteasome is limiting, the rate of substrate degradation would be determined by the proteasome level and would lead to a linear decline in protein level instead of the more exponential decay we observed. Thus we believe such an assumption is fair. Given all these caveats, we still provided useful insights to understand the system, and our model could serve as a starting point for a more sophisticated system.

Figure 13

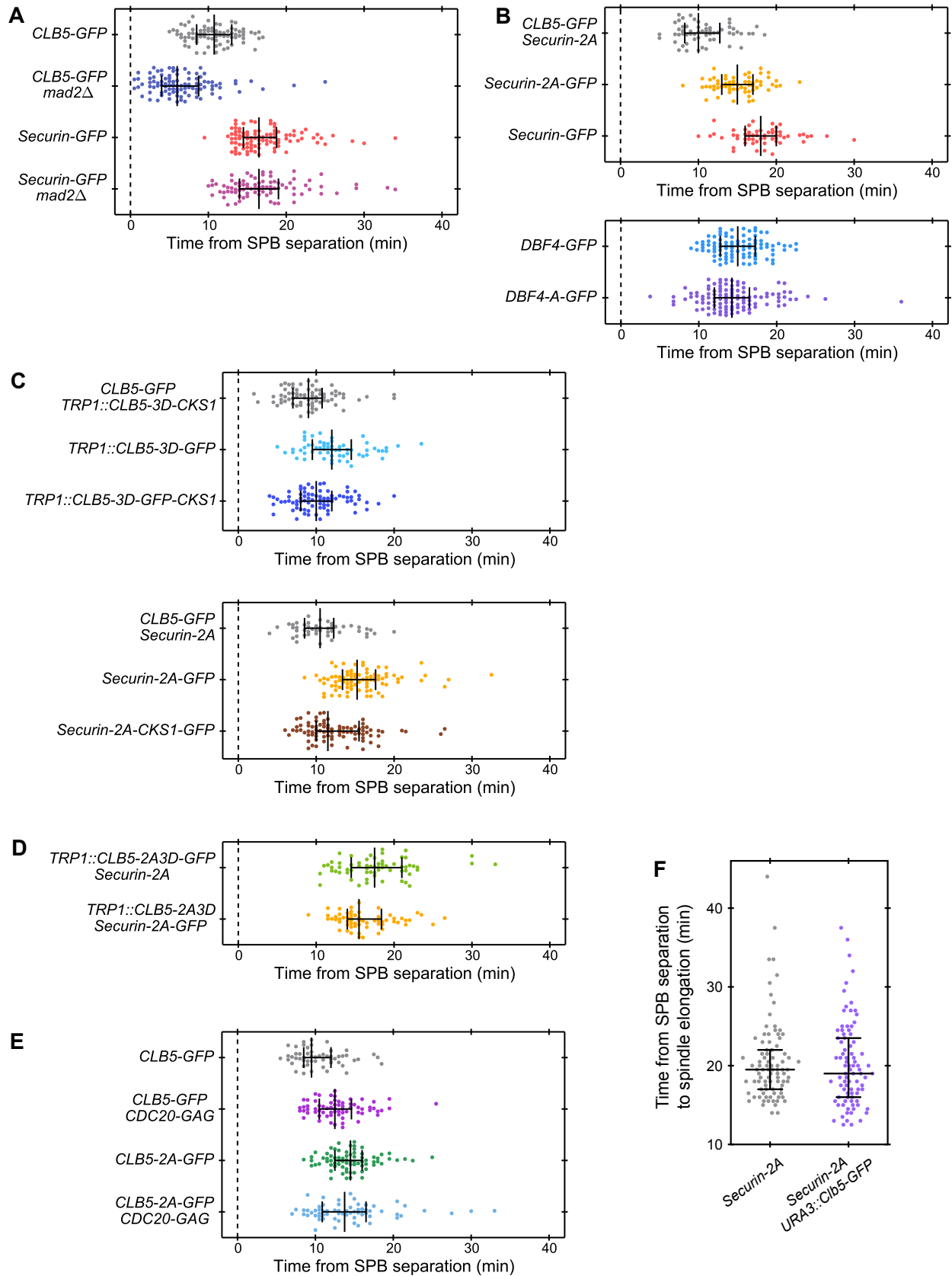
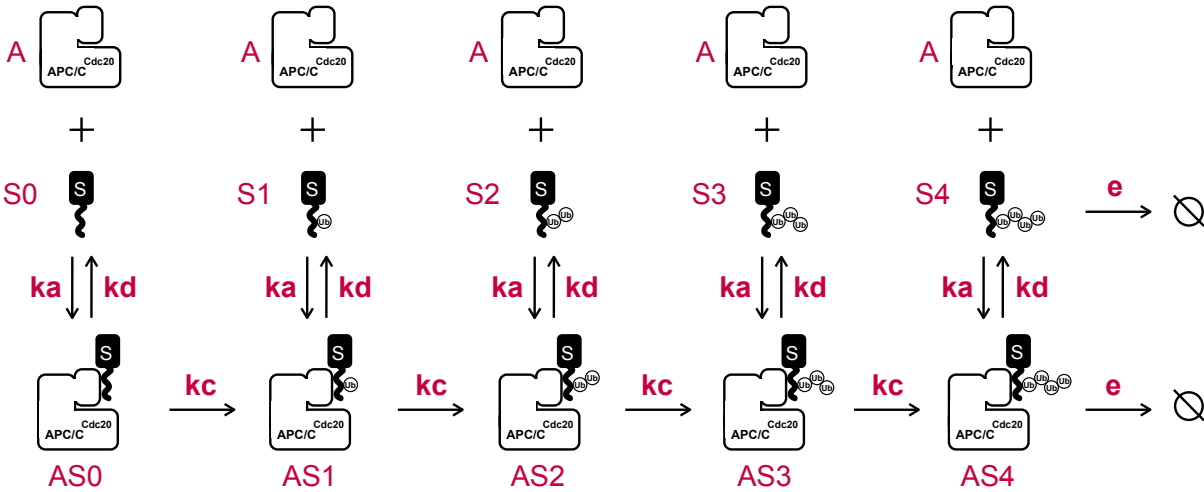


Figure 13. **Timing of degradation onset for different strains.** (A) shows the same strains in Fig. 3A. (B) shows the same strains in Fig. 4A and 4E. (C) shows the same strains in Fig. 5B and 5C. (D) shows the same strains in Fig. 6C. (E) shows the same strains in Fig. 6D. (F) Anaphase onset in securin-2A strains with one or two copies of Clb5.

Figure 14

A



B

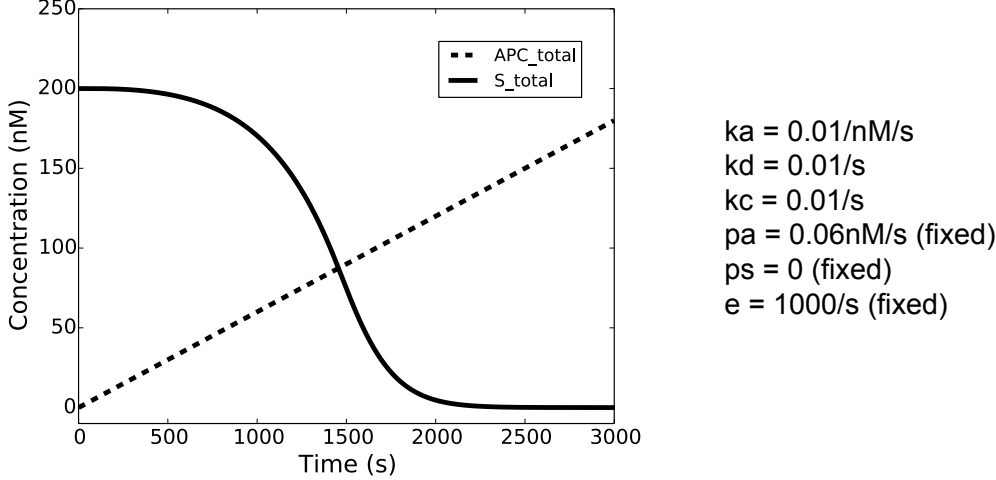


Figure 14. **A dynamic model for APC-substrate interaction.** (A) Components of the model. A: free APC/C, S: free substrate, AS: APC/C-substrate complex, k_a : association rate, k_d : dissociation rate, k_c : catalytic rate, e : degradation rate. (B) The degradation profile of substrate at a given parameter set. p_a : activation rate of APC, p_s : production rate of substrate.

Figure 15

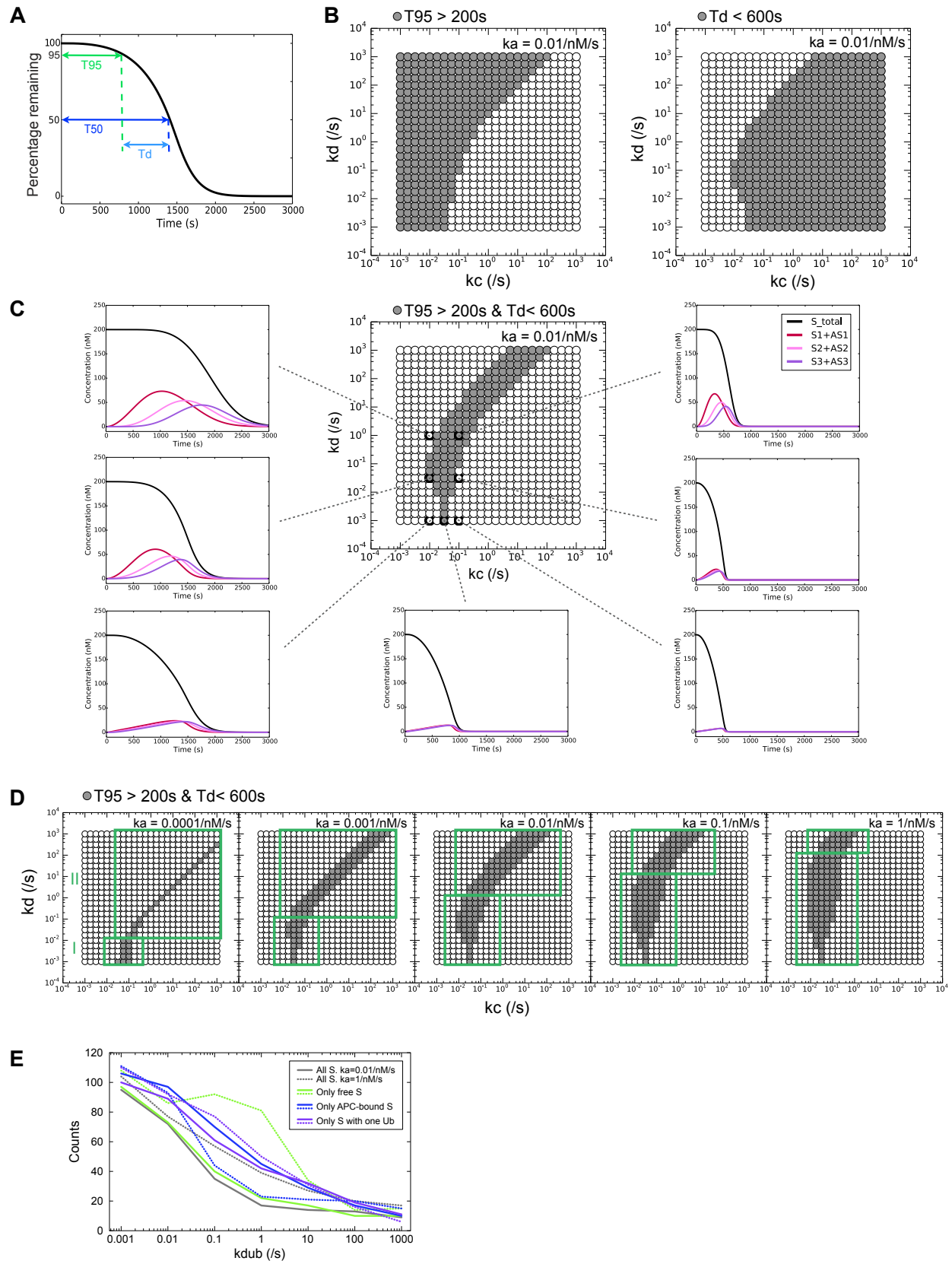


Figure 15. The delay in degradation onset and rate of degradation varies with parameters.

(A) Measurement of T_{95} as an estimate of the delay in degradation onset, and T_d as an estimate of degradation rate. (B) The k_c - k_d parameter regions where $T_{95} > 200s$ or $T_d < 600s$ (grey). $k_a = 0.01/nM/s$. (C) The parameter region where $T_{95} > 200s$ and $T_d < 600s$ (grey), and the substrate degradation profile with different parameters. Purple and pink lines show the intermediate products with one, two or three ubiquitins attached. $k_a = 0.01/nM/s$ (D) The parameter region that meets T_{95} and T_d requirements varies with k_a , and is consisted of Region I and II (green boxes). (E) At $k_a = 0.01/nM/s$ (solid lines) and $k_a = 1/nM/s$ (dash lines), the number of parameter combinations that meet the T_{95} and T_d requirements as a function of deubiquitination rate k_{dub} , in different deubiquitination scenarios.

Figure 16

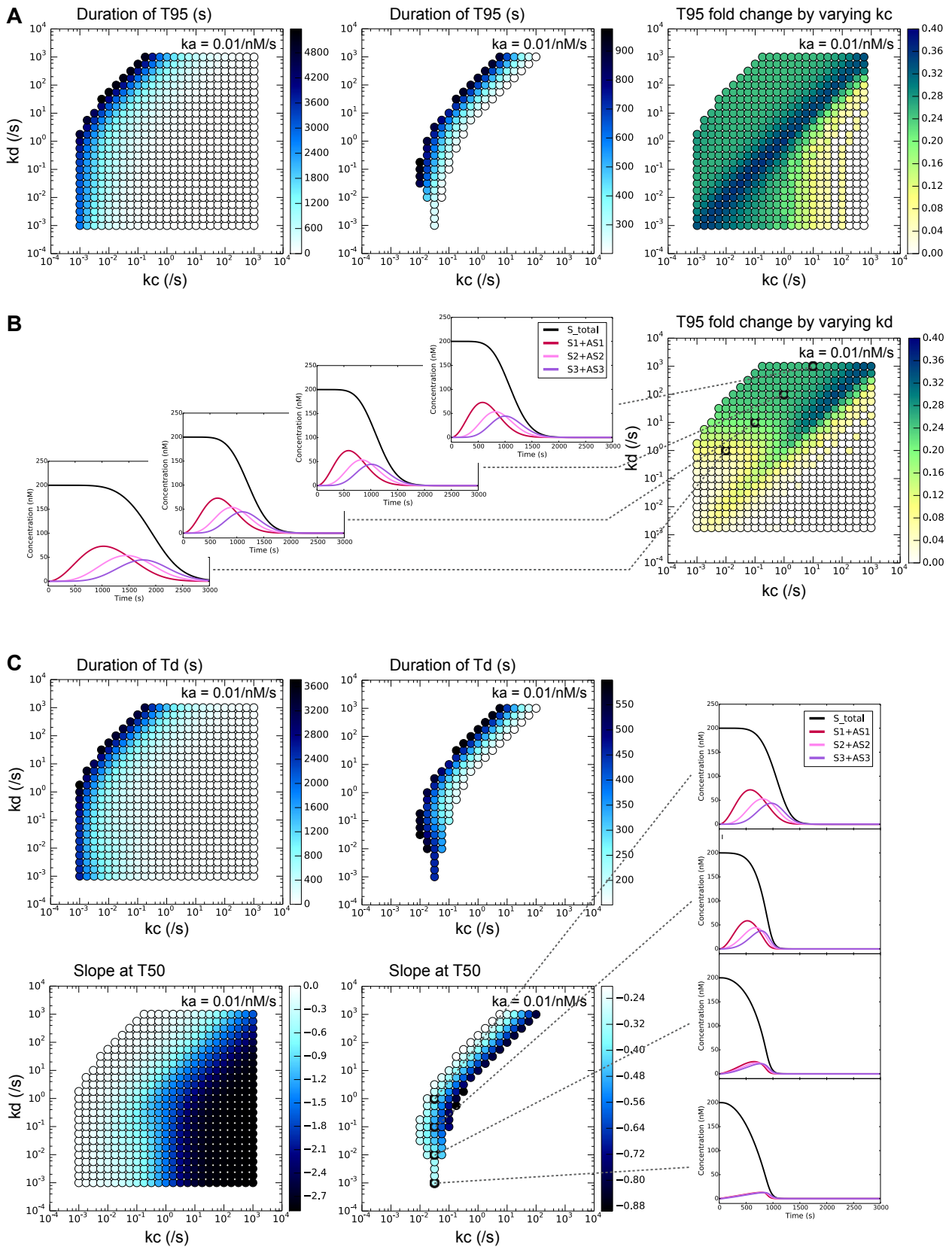
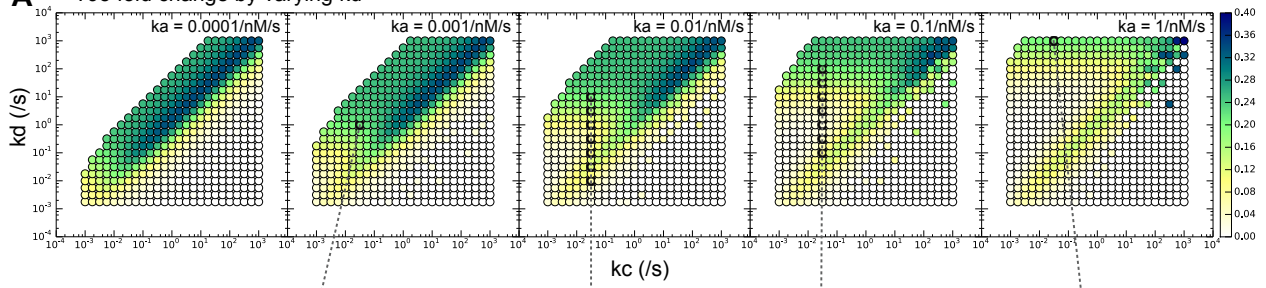


Figure 16. **Impact of k_c and k_d on T95 and Td.** (A) Left panel: duration of T95 at different k_c and k_d . Middle panel: the value of T95 in the parameter region that meets T95 and Td requirements. Right panel: change of T95 when increasing k_c by 1.8 fold, normalized by the absolute value of T95. (B) Left: degradation profile in different parameter regions, showing that in the green region, increasing k_c and meanwhile increasing k_d compensate for each other. Right: change of T95 when decreasing k_d by 1.8 fold, normalized by the absolute value of T95. (C) Top: duration of Td at different k_c and k_d . Bottom: the slope at T50, as an estimate of the fastest degradation rate, at different k_c and k_d . Right: degradation profiles showing that in certain regions increasing k_d does not significantly increase T95 but instead increases the rate of degradation. In all panels $k_a = 0.01/\text{nM/s}$.

Figure 17

A T95 fold change by varying k_d



B

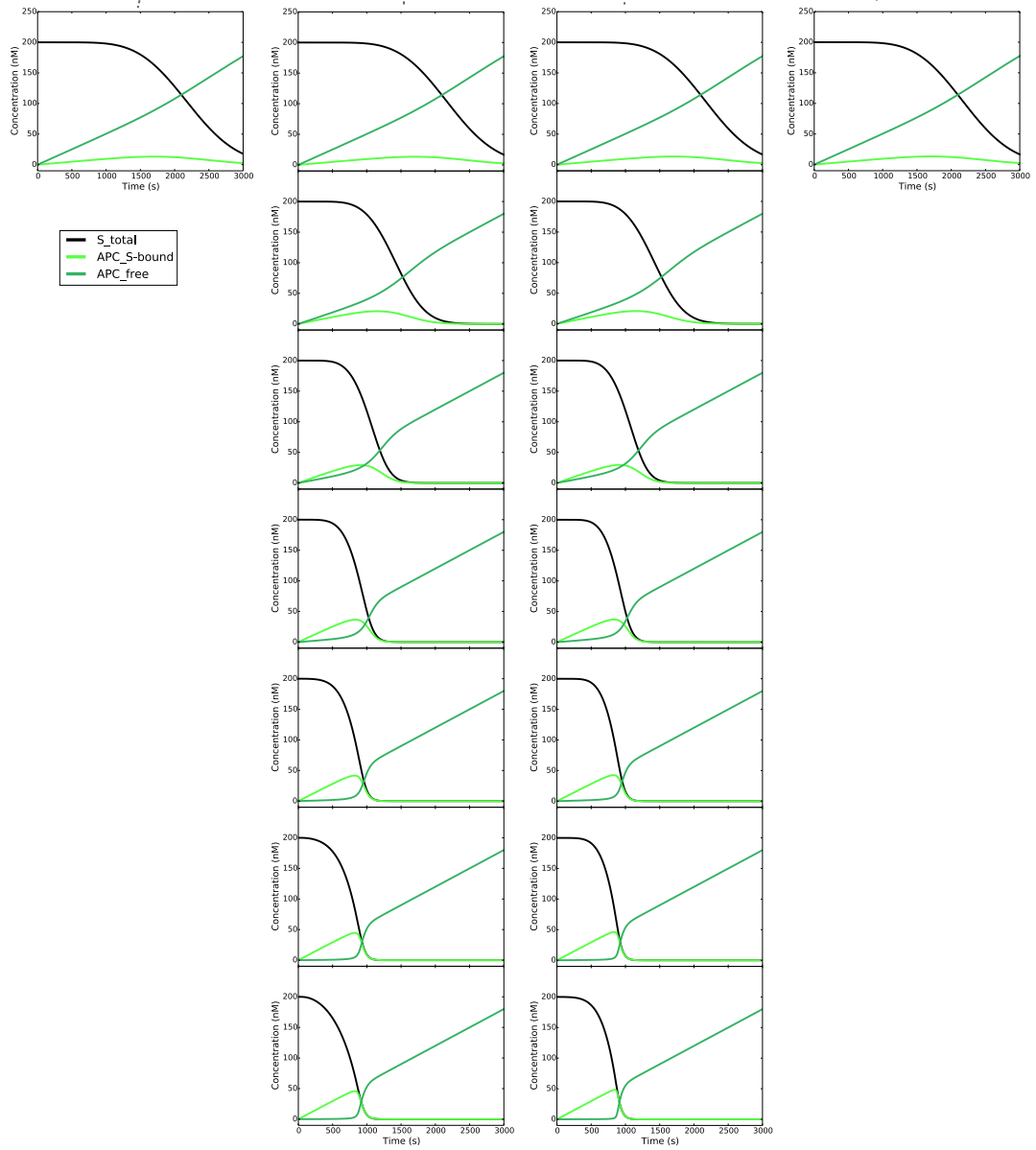


Figure 17. **The region where changing k_d significantly influences T95 varies with k_a .** (A) Fold change of T95 when decreasing k_d by 1.8 fold at different k_a . (B) Degradation profiles showing that increasing k_d leads to significant change of T95 only when there is enough free APC in the system, which is determined by a combination of k_d and k_a .

Figure 18

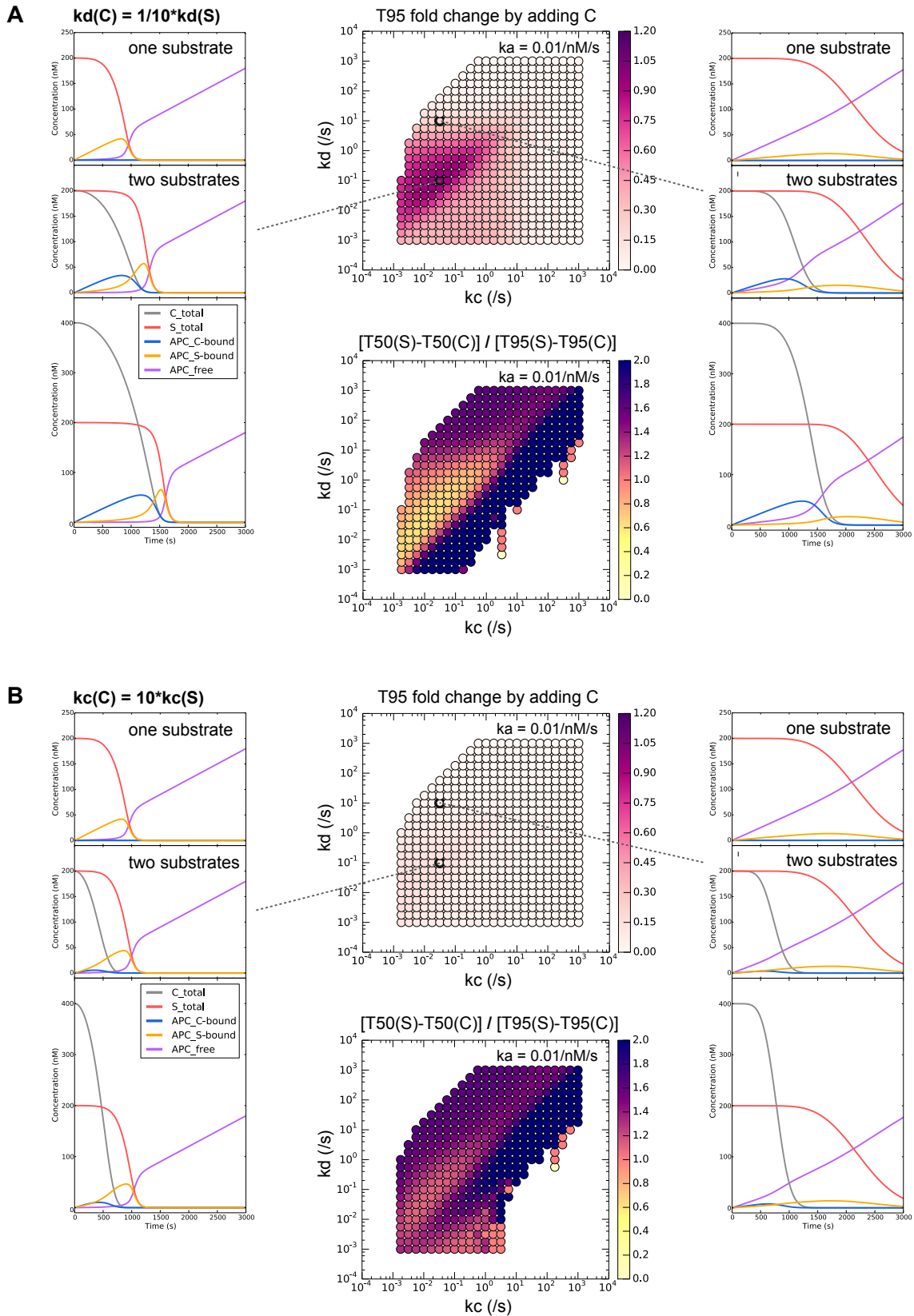


Figure 18. **Impact of adding a second substrate C.** (A) C has a dissociation rate k_d 10 times smaller than S. Left panel: from top to bottom: degradation profiles of one-substrate system, two-substrate system starting with equal concentration of C and S, and starting from C with twice the concentration of S. Center top: change in T95 of S after adding equal concentration of C, normalized by T95 without C. Center bottom: in a system starting from equal concentration of C and S, the difference of T50 between the two substrates as a ratio of the difference of T95. Right panel: the same as left panel. (B) C has a catalytic rate k_c 10 times faster than S. Panels are arranged the same way as in (A).

Table 1. Yeast strains used in this study.

Strain	Genotype	Figure
DOM90	Wild-type W303 (AFS92, A. Straight): <i>MATa</i> , <i>bar1::HisG</i>	
DL00S	<i>spc42::SPC42-mCherry-HIS3</i> DOM90 (parent strain of all following strains)	Figure 2A, 11D,E
DL009C	<i>clb5::CLB5-GFP-URA3</i>	Figure 1B 2A-D 3A,B 6B,D,F 9A,B 11A
DL009P	<i>pds1::PDS1-GFP-URA3</i>	Figure 1B 2A-D, 3A,C 9A,B 10A
DL103	<i>dbf4::DBF4-GFP-URA3</i>	Figure 1B 2A-D 4E, 10C
DL029	<i>clb2::CLB2-GFP-URA3</i>	Figure 1B 2A-D
DL072	<i>mad2::NATMX clb5::CLB5-GFP-URA3</i>	Figure 3A,D 9A,B
DL073	<i>mad2::NATMX pds1::PDS1-GFP-URA3</i>	Figure 3A,D 9A,B
DL128	<i>cdc20::NAT-prGALS-CDC20 clb5::CLB5-GFP-URA3</i>	Figure 3E
DL122	<i>pds1::PDS1-GFP-KanMX ura3::URA3</i>	Figure 4A,B 10A
DL123	<i>pds1::PDS1-2A-GFP-KanMX ura3::URA3</i>	Figure 4A,B 8A 10A,D
DL108	<i>pds1::PDS1-2A-KANMX clb5::CLB5-GFP-URA3</i>	Figure 4A, 5C 8A 12C
DL206	<i>dbf4::DBF4-A-GFP-URA3</i>	Figure 4E, 10C
DL159	<i>trp1::pCLB5-CLB5-3D-GFP-TRP1</i>	Figure 5B, 11E
DL215	<i>trp1::pCLB5-CLB5-3D-GFP-CKS1-TRP1</i>	Figure 5B
DL216	<i>trp1::pCLB5-CLB5-3D-CKS1-TRP1 clb5::CLB5-GFP-URA3</i>	Figure 5B
DL199	<i>pds1::PDS1-2A-CKS1-GFP-KANMX</i>	Figure 5C,D 12B
DL200	<i>pds1::PDS1-2A-CKS1-KANMX clb5::CLB5-GFP-URA3</i>	Figure 5C
DL015	<i>pds1::PDS1-2A-GFP-KanMX</i>	Figure 5C,D 12B
DL202	<i>clb5::CLB5-2A-GFP-URA3</i>	Figure 6B,D,F
DL203	<i>trp1::pCLB5-CLB5-2A3D-TRP1 pds1::PDS1-2A-GFP-KANMX</i>	Figure 6C
DL204	<i>trp1::pCLB5-CLB5-2A3D-GFP-TRP1 pds1::PDS1-2A</i>	Figure 6C
DL209	<i>cdc20::CDC20-GAG-NATMX clb5::CLB5-GFP-URA3</i>	Figure 6D
DL210	<i>cdc20::CDC20-GAG-NATMX clb5::CLB5-2A-URA3</i>	Figure 6D
DL130	<i>mad1::NATMX clb5::CLB5-GFP-URA3</i>	Figure 9A,B
DL131	<i>mad1::NATMX pds1::PDS1-GFP-URA3</i>	Figure 9A,B
DL125	<i>chk1::NATMX ura3::URA3 pds1::PDS1-2A-GFP-KANMX</i>	Figure 10D
DL061	<i>clb5::PDS1-2A-N-CLB5C-GFP-URA3</i>	Figure 11A
DL143	<i>trp1::pCLB5-CLB5delN-I166D,F291D-GFP-TRP1</i>	Figure 11D,E
DL144	<i>trp1::pCLB5-CLB5delN-I166D,F291R-GFP-TRP1</i>	Figure 11D,E
DL145	<i>trp1::pCLB5-CLB5delN-F169D,F291D-GFP-TRP1</i>	Figure 11D
DL146	<i>trp1::pCLB5-CLB5delN-F169D,F291R-GFP-TRP1</i>	Figure 11D
DL147	<i>trp1::pCLB5-CLB5delN-I166D, F254D, F291D-GFP-TRP1</i>	Figure 11D,E
DL148	<i>trp1::pCLB5-CLB5delN-I166D, F254D, F291R-GFP-TRP1</i>	Figure 11D
DL151	<i>trp1::pCLB5-CLB5delN-3D-GFP-TRP1</i>	Figure 11D,E
DL166	<i>trp1::pCLB5-CLB5delN-I166D, F169A, F254D, F291D-GFP-TRP1</i>	Figure 11E
DL165	<i>trp1::pCLB5-CLB5-GFP-TRP1</i>	Figure 11E
DL154	<i>trp1::pCLB5-CLB5-I166D,F291D-GFP-TRP1</i>	Figure 11E
DL155	<i>trp1::pCLB5-CLB5-I166D,F291R-GFP-TRP1</i>	Figure 11E
DL156	<i>trp1::pCLB5-CLB5-F169D,F291D-GFP-TRP1</i>	Figure 11E
DL157	<i>trp1::pCLB5-CLB5-I166D, F254D, F291D-GFP-TRP1</i>	Figure 11E
DL164	<i>trp1::pCLB5-CLB5-3D-GFP-TRP1 cdc20::NATMX-pGALS-CDC20</i>	Figure 12A
DL170	<i>trp1::pCLB5-CLB5-3D-TRP1 pds1::PDS1-2A-GFP-KANMX</i>	Figure 12C
DL173	<i>trp1::pCLB5-CLB5-3D-GFP-TRP1 pds1::PDS1-2A</i>	Figure 12C
DL249	<i>pds1::PDS1-2A ura3::URA3</i>	Figure 13F
DL250	<i>pds1::PDS1-2A ura3::CLB5-GFP-URA3</i>	Figure 13F

CHAPTER 4. CONCLUSION

A more complete picture of APC/C^{Cdc20} substrate degradation emerges from these studies. Its substrates Clb5, securin, Dbf4 and Clb2 are degraded sequentially in mitosis. Clb5 can be degraded earlier than other substrates due to its interaction with the Cdk1-Cks1 complex, which bridges it to the APC/C core complex, and its ABBA motif which represents a novel Cdc20-binding motif. Dbf4 and securin are phosphorylated by Cdk1 near their D box and KEN box, and that delays their degradation. Agreeing with previous measurements made in the population level, Clb2 degradation is initiated by APC/C^{Cdc20} and later completed by APC/C^{Cdh1}. It remains unclear how after partial degradation by APC/C^{Cdc20}, Clb2 can be stabilized even though APC/C^{Cdc20} is still actively ubiquitinating securin at that time.

The timing difference of their degradation is unlikely due to competition among substrates. Instead, substrates degrade at distinct timing due to the different time duration they need to acquire enough ubiquitins for efficient degradation. Those mechanisms above modulate this time duration likely by influencing binding affinity for APC/C^{Cdc20}, and/or the ability for substrate-bound Cdc20 to activate APC/C for ubiquitin transfer. To understand exactly what they do and how they do it requires future efforts.

REFERENCES

- Agarwal, R., Z. Tang, H. Yu, and O. Cohen-Fix. 2003. Two distinct pathways for inhibiting pds1 ubiquitination in response to DNA damage. *J. Biol. Chem.* 278:45027-45033.
- Alexandru, G., F. Uhlmann, K. Mechtler, M.A. Poupart, and K. Nasmyth. 2001. Phosphorylation of the cohesin subunit Scc1 by Polo/Cdc5 kinase regulates sister chromatid separation in yeast. *Cell.* 105:459-472.
- Barford, D. 2011. Structure, function and mechanism of the anaphase promoting complex (APC/C). *Q. Rev. Biophys.* 44:153-190.
- Baudin, A., O. Ozier-Kalogeropoulos, A. Denouel, F. Lacroute, and C. Cullin. 1993. A simple and efficient method for direct gene deletion in *Saccharomyces cerevisiae*. *Nucleic Acids Res.* 21:3329-3330.
- Baumer, M., G.H. Braus, and S. Irniger. 2000. Two different modes of cyclin clb2 proteolysis during mitosis in *Saccharomyces cerevisiae*. *FEBS Lett.* 468:142-148.
- Bell, S.P., and A. Dutta. 2002. DNA replication in eukaryotic cells. *Annu. Rev. Biochem.* 71:333-374.
- Bock, L.J., C. Pagliuca, N. Kobayashi, R.A. Grove, Y. Oku, K. Shrestha, C. Alfieri, C. Golfieri, A. Oldani, M. Dal Maschio, R. Bermejo, T.R. Hazbun, T.U. Tanaka, and P. De Wulf. 2012. Cnn1 inhibits the interactions between the KMN complexes of the yeast kinetochore. *Nat. Cell Biol.* 14:614-624.
- Bouchoux, C., and F. Uhlmann. 2011. A quantitative model for ordered Cdk substrate dephosphorylation during mitotic exit. *Cell.* 147:803-814.
- Brizuela, L., G. Draetta, and D. Beach. 1987. p13^{suc1} acts in the fission yeast cell division cycle as a component of the p34^{cdc2} protein kinase. *EMBO J.* 6:3507-3514.

- Brown, N.R., E.D. Lowe, E. Petri, V. Skamnaki, R. Antrobus, and L.N. Johnson. 2007. Cyclin B and cyclin A confer different substrate recognition properties on CDK2. *Cell Cycle*. 6:1350-1359.
- Burton, J.L., Y. Xiong, and M.J. Solomon. 2011. Mechanisms of pseudosubstrate inhibition of the anaphase promoting complex by Acm1. *EMBO J*. 30:1818-1829.
- Carroll, C.W., and Morgan, D.O. 2002. The Doc1 subunit is a processivity factor for the anaphase-promoting complex. *Nat. Cell Biol*. 4:880-887.
- Carroll, C.W., M. Enquist-Newman, and D.O. Morgan. 2005. The APC subunit Doc1 promotes recognition of the substrate destruction box. *Current biology*. 15:11-18.
- Chang, L., Z. Zhang, J. Yang, S.H. McLaughlin, and D. Barford. 2014. Molecular architecture and mechanism of the anaphase-promoting complex. *Nature*. 513:388-393.
- Clute, P., and J. Pines. 1999. Temporal and spatial control of cyclin B1 destruction in metaphase. *Nat. Cell Biol*. 1:82-87.
- Collin, P., O. Nashchekina, R. Walker, and J. Pines. 2013. The spindle assembly checkpoint works like a rheostat rather than a toggle switch. *Nat. Cell Biol*. 15:1378-1385.
- Crocker, J.C., and D.G. Grier. 1996. Methods of digital video microscopy for colloidal studies. *J Colloid Interf Sci*. 179:298-310.
- Davey, N.E., J.L. Cowan, D.C. Shields, T.J. Gibson, M.J. Coldwell, and R.J. Edwards. 2012. SLiMPrints: conservation-based discovery of functional motif fingerprints in intrinsically disordered protein regions. *Nucleic Acids Res*. 40:10628-10641.
- den Elzen, N., and J. Pines. 2001. Cyclin A is destroyed in prometaphase and can delay chromosome alignment and anaphase. *J. Cell Biol*. 153:121-136.
- Di Fiore, B., and J. Pines. 2010. How cyclin A destruction escapes the spindle assembly

- checkpoint. *J. Cell Biol.* 190:501-509.
- Dick, A.E., and D.W. Gerlich. 2013. Kinetic framework of spindle assembly checkpoint signalling. *Nat. Cell Biol.* 15:1370-1377.
- Edelstein, A., N. Amodaj, K. Hoover, R. Vale, and N. Stuurman. 2010. Computer control of microscopes using microManager. *Curr. Prot. Mol. Biol.* Chapter 14:Unit14 20.
- Enquist-Newman, M., M. Sullivan, and D.O. Morgan. 2008. Modulation of the mitotic regulatory network by APC-dependent destruction of the Cdh1 inhibitor Acm1. *Mol. Cell.* 30:437-446.
- Fang, G., H. Yu, and M.W. Kirschner. 1998. Direct binding of CDC20 protein family members activates the anaphase-promoting complex in mitosis and G1. *Molecular cell.* 2:163-171.
- Ferreira, M.F., C. Santocanale, L.S. Drury, and J.F. Diffley. 2000. Dbf4p, an essential S phase-promoting factor, is targeted for degradation by the anaphase-promoting complex. *Mol. Cell. Biol.* 20:242-248.
- Foster, S.A., and D.O. Morgan. 2012. The APC/C subunit Mnd2/Apc15 promotes Cdc20 autoubiquitination and spindle assembly checkpoint inactivation. *Mol. Cell.* 47:921-932.
- Fukuhara, N., and T. Kawabata. 2008. HOMCOS: a server to predict interacting protein pairs and interacting sites by homology modeling of complex structures. *Nucleic Acids Res.* 36:W185-189.
- Geley, S., E. Kramer, C. Gieffers, J. Gannon, J.M. Peters, and T. Hunt. 2001. Anaphase-promoting complex/cyclosome-dependent proteolysis of human cyclin A starts at the beginning of mitosis and is not subject to the spindle assembly checkpoint. *J. Cell Biol.* 153:137-148.
- Ghaemmaghami, S., W.K. Huh, K. Bower, R.W. Howson, A. Belle, N. Dephoure, E.K. O'Shea,

- and J.S. Weissman. 2003. Global analysis of protein expression in yeast. *Nature*. 425:737-741.
- Glickman, M.H., and A. Ciechanover. 2002. The ubiquitin-proteasome proteolytic pathway: destruction for the sake of construction. *Physiological reviews*. 82:373-428.
- Glotzer, M., A.W. Murray, and M.W. Kirschner. 1991. Cyclin is degraded by the ubiquitin pathway. *Nature*. 349:132-138.
- Goldstein, A.L., and J.H. McCusker. 1999. Three new dominant drug resistance cassettes for gene disruption in *Saccharomyces cerevisiae*. *Yeast*. 15:1541-1553.
- Goshima, G., and M. Yanagida. 2000. Establishing biorientation occurs with precocious separation of the sister kinetochores, but not the arms, in the early spindle of budding yeast. *Cell*. 100:619-633.
- Hadwiger, J.A., C. Wittenberg, M.D. Mendenhall, and S.I. Reed. 1989. The *Saccharomyces cerevisiae* CKS1 gene, a homolog of the *Schizosaccharomyces pombe* *suc1+* gene, encodes a subunit of the Cdc28 protein kinase complex. *Mol. Cell. Biol.* 9:2034-2041.
- Hagting, A., N. Den Elzen, H.C. Vodermaier, I.C. Waizenegger, J.M. Peters, and J. Pines. 2002. Human securin proteolysis is controlled by the spindle checkpoint and reveals when the APC/C switches from activation by Cdc20 to Cdh1. *J. Cell Biol.* 157:1125-1137.
- Hames, R.S., S.L. Wattam, H. Yamano, R. Bacchieri, and A.M. Fry. 2001. APC/C-mediated destruction of the centrosomal kinase Nek2A occurs in early mitosis and depends upon a cyclin A-type D-box. *EMBO J.* 20:7117-7127.
- Hayes, M.J., Y. Kimata, S.L. Wattam, C. Lindon, G. Mao, H. Yamano, and A.M. Fry. 2006. Early mitotic degradation of Nek2A depends on Cdc20-independent interaction with the APC/C. *Nat. Cell Biol.* 8:607-614.

- He, J., W.C.H. Chao, Z. Zhang, J. Yang, N. Cronin, and D. Barford. 2013. Insights into degron recognition by APC/C coactivators from the structure of an Acm1-Cdh1 complex. *Mol. Cell.* 50:649-660.
- He, X., S. Asthana, and P.K. Sorger. 2000. Transient sister chromatid separation and elastic deformation of chromosomes during mitosis in budding yeast. *Cell.* 101:763-775.
- Holt, L.J., A.N. Krutchinsky, and D.O. Morgan. 2008. Positive feedback sharpens the anaphase switch. *Nature.* 454:353-357.
- Holt, L.J., B.B. Tuch, J. Villen, A.D. Johnson, S.P. Gygi, and D.O. Morgan. 2009. Global analysis of Cdk1 substrate phosphorylation sites provides insights into evolution. *Science.* 325:1682-1686.
- Honda, R., E.D. Lowe, E. Dubinina, V. Skamnaki, A. Cook, N.R. Brown, and L.N. Johnson. 2005. The structure of cyclin E1/CDK2: implications for CDK2 activation and CDK2-independent roles. *EMBO J.* 24:452-463.
- Hoyt, M.A., L. Totis, and B.T. Roberts. 1991. *S. cerevisiae* genes required for cell cycle arrest in response to microtubule function. *Cell.* 66:507-517.
- Hunter, J.D. 2007. Matplotlib: A 2D graphics environment. *Comput. Sci. Eng.* 9:90-95.
- Jansen, G., C. Wu, B. Schade, D.Y. Thomas, and M. Whiteway. 2005. Drag&Drop cloning in yeast. *Gene.* 344:43-51.
- Jaspersen, S.L., J.F. Charles, and D.O. Morgan. 1999. Inhibitory phosphorylation of the APC regulator Hct1 is controlled by the kinase Cdc28 and the phosphatase Cdc14. *Curr. Biol.* 9:227-236.
- Jeffrey, P.D., A.A. Russo, K. Polyak, E. Gibbs, J. Hurwitz, J. Massague, and N.P. Pavletich. 1995. Mechanism of CDK activation revealed by the structure of a cyclin A-CDK2

- complex. *Nature*. 376:313-320.
- Juang, Y.-L., J. Huang, J.-M. Peters, M.E. McLaughlin, C.-Y. Tai, and D. Pellman. 1997. APC-mediated proteolysis of Ase1 and the morphogenesis of the mitotic spindle. *Science*. 275:1311-1314.
- Kabeche, L., and D.A. Compton. 2013. Cyclin A regulates kinetochore microtubules to promote faithful chromosome segregation. *Nature*. 502:110-113.
- Keyes, B.E., C.M. Yellman, and D.J. Burke. 2008. Differential regulation of anaphase promoting complex/cyclosome substrates by the spindle assembly checkpoint in *Saccharomyces cerevisiae*. *Genetics*. 178:589-591.
- Khmelniskii, A., J. Roostalu, H. Roque, C. Antony, and E. Schiebel. 2009. Phosphorylation-dependent protein interactions at the spindle midzone mediate cell cycle regulation of spindle elongation. *Dev. Cell*. 17:244-256.
- Kilmartin, J.V., S.L. Dyos, D. Kershaw, and J.T. Finch. 1993. A spacer protein in the *Saccharomyces cerevisiae* spindle pole body whose transcript is cell cycle-regulated. *J. Cell Biol.* 123:1175-1184.
- Kõivomägi, M., M. Ord, A. Iofik, E. Valk, R. Venta, I. Faustova, R. Kivi, E.R. Balog, S.M. Rubin, and M. Loog. 2013. Multisite phosphorylation networks as signal processors for Cdk1. *Nat. Struct. Mol. Biol.* 20:1415-1424.
- Kraft, C., F. Herzog, C. Gieffers, K. Mechtler, A. Hagting, J. Pines, and J.M. Peters. 2003. Mitotic regulation of the human anaphase-promoting complex by phosphorylation. *EMBO J.* 22:6598-6609.
- Kramer, E.R., C. Gieffers, G. Holzl, M. Hengstschlager, and J.M. Peters. 1998. Activation of the human anaphase-promoting complex by proteins of the CDC20/Fizzy family. *Current*

- biology*. 8:1207-1210.
- Lara-Gonzalez, P., F.G. Westhorpe, and S.S. Taylor. 2012. The spindle assembly checkpoint. *Curr. Biol.* 22:R966-980.
- Li, R., and A.W. Murray. 1991. Feedback control of mitosis in budding yeast. *Cell*. 66:519-531.
- Liang, N., E.C. Williams, E.K. Kennedy, C. Dore, S. Pilon, S.L. Girard, J.S. Deneault, and A.D. Rudner. 2013. A Wee1 checkpoint inhibits anaphase onset. *J. Cell Biol.* 201:843-862.
- Longtine, M.S., A. McKenzie, D.J. Demarini, N.G. Shah, A. Wach, A. Brachat, P. Philippsen, and J.R. Pringle. 1998. Additional modules for versatile and economical PCR-based gene deletion and modification in *Saccharomyces cerevisiae*. *Yeast*. 14:953-961.
- Loog, M., and D.O. Morgan. 2005. Cyclin specificity in the phosphorylation of cyclin-dependent kinase substrates. *Nature*. 434:104-108.
- Matyskiela, M.E., and D.O. Morgan. 2009. Analysis of activator-binding sites on the APC/C supports a cooperative substrate-binding mechanism. *Mol. Cell*. 34:68-80.
- Matyskiela, M.E., M.C. Rodrigo-Brenni, and D.O. Morgan. 2009. Mechanisms of ubiquitin transfer by the anaphase-promoting complex. *Journal of biology*. 8:92.
- McGrath, D.A., E.R. Balog, M. Koivomagi, R. Lucena, M.V. Mai, A. Hirschi, D.R. Kellogg, M. Loog, and S.M. Rubin. 2013. Cks confers specificity to phosphorylation-dependent CDK signaling pathways. *Nat. Struct. Mol. Biol.*
- Meraldi, P., V.M. Draviam, and P.K. Sorger. 2004. Timing and checkpoints in the regulation of mitotic progression. *Dev. Cell*. 7:45-60.
- Michel, L., E. Diaz-Rodriguez, G. Narayan, E. Hernando, V.V. Murty, and R. Benezra. 2004. Complete loss of the tumor suppressor MAD2 causes premature cyclin B degradation and mitotic failure in human somatic cells. *Proc. Natl. Acad. Sci. U. S. A.* 101:4459-4464.

- Michel, L.S., V. Liberal, A. Chatterjee, R. Kirchwegger, B. Pasche, W. Gerald, M. Dobles, P.K. Sorger, V.V. Murty, and R. Benezra. 2001. MAD2 haplo-insufficiency causes premature anaphase and chromosome instability in mammalian cells. *Nature*. 409:355-359.
- Morgan, D.O. 2007. *The Cell Cycle: Principles of Control*. New Science Press, London.
- Mumberg, D., R. Muller, and M. Funk. 1994. Regulatable promoters of *Saccharomyces cerevisiae*: comparison of transcriptional activity and their use for heterologous expression. *Nucleic Acids Res.* 22:5767-5768.
- Musacchio, A., and E.D. Salmon. 2007. The spindle-assembly checkpoint in space and time. *Nat. Rev. Mol. Cell Biol.* 8:379-393.
- Nasmyth, K., and C.H. Haering. 2009. Cohesin: its roles and mechanisms. *Annu. Rev. Genet.* 43:525-558.
- Oliphant, T.E. 2007. Python for scientific computing. *Comput. Sci. Eng.* 9:10-20.
- Oshiro, G., J.C. Owens, Y. Shellman, R.A. Sclafani, and J.J. Li. 1999. Cell cycle control of Cdc7p kinase activity through regulation of Dbf4p stability. *Mol. Cell. Biol.* 19:4888-4896.
- Patra, D., and W.G. Dunphy. 1998. Xe-p9, a *Xenopus* Suc1/Cks protein, is essential for the Cdc2-dependent phosphorylation of the anaphase-promoting complex at mitosis. *Genes Dev.* 12:2549-2559.
- Pearson, C.G., P.S. Maddox, E.D. Salmon, and K. Bloom. 2001. Budding yeast chromosome structure and dynamics during mitosis. *J. Cell Biol.* 152:1255-1266.
- Peters, J.M. 2006. The anaphase promoting complex/cyclosome: a machine designed to destroy. *Nat. Rev. Mol. Cell Biol.* 7:644-656.
- Pettersen, E.F., T.D. Goddard, C.C. Huang, G.S. Couch, D.M. Greenblatt, E.C. Meng, and T.E.

- Ferrin. 2004. UCSF Chimera--a visualization system for exploratory research and analysis. *J. Comp. Chem.* 25:1605-1612.
- Pfleger, C.M., and M.W. Kirschner. 2000. The KEN box: an APC recognition signal distinct from the D box targeted by Cdh1. *Genes Dev.* 14:655-665.
- Pines, J. 2006. Mitosis: a matter of getting rid of the right protein at the right time. *Trends Cell Biol.* 16:55-63.
- Pines, J. 2011. Cubism and the cell cycle: the many faces of the APC/C. *Nat. Rev. Mol. Cell Biol.* 12:427-438.
- Primorac, I., and A. Musacchio. 2013. Panta rhei: The APC/C at steady state. *J. Cell Biol.* 201:177-189.
- Queralt, E., C. Lehane, B. Novak, and F. Uhlmann. 2006. Downregulation of PP2A(Cdc55) phosphatase by separase initiates mitotic exit in budding yeast. *Cell.* 125:719-732.
- Queralt, E., and F. Uhlmann. 2008. Cdk-counteracting phosphatases unlock mitotic exit. *Curr. Opin. Cell Biol.* 20:661-668.
- Richardson, H.E., C.S. Stueland, J. Thomas, P. Russell, and S.I. Reed. 1990. Human cDNAs encoding homologs of the small p34^{Cdc28/Cdc2}-associated protein of *Saccharomyces cerevisiae* and *Schizosaccharomyces pombe*. *Genes Dev.* 4:1332-1344.
- Rodrigo-Brenni, M.C., and D.O. Morgan. 2007. Sequential E2s drive polyubiquitin chain assembly on APC targets. *Cell.* 130:127-139.
- Rothbauer, U., K. Zolghadr, S. Muyldermans, A. Schepers, M.C. Cardoso, and H. Leonhardt. 2008. A versatile nanotrapp for biochemical and functional studies with fluorescent fusion proteins. *Mol. Cell Proteomics.* 7:282-289.
- Rudner, A.D., and A.W. Murray. 2000. Phosphorylation by Cdc28 activates the Cdc20-dependent

- activity of the anaphase-promoting complex. *J. Cell Biol.* 149:1377-1390.
- Russo, A.A., P.D. Jeffrey, and N.P. Pavletich. 1996. Structural basis of cyclin-dependent kinase activation by phosphorylation. *Nat. Struct. Biol.* 3:696-700.
- Schaefer, J.B., and D.O. Morgan. 2011. Protein-linked ubiquitin chain structure restricts activity of deubiquitinating enzymes. *J. Bio. Chem.* 286:45186-45196.
- Schleiffer, A., M. Maier, G. Litos, F. Lampert, P. Hornung, K. Mechtler, and S. Westermann. 2012. CENP-T proteins are conserved centromere receptors of the Ndc80 complex. *Nat. Cell Biol.* 14:604-613.
- Schneider, C.A., W.S. Rasband, and K.W. Eliceiri. 2012. NIH Image to ImageJ: 25 years of image analysis. *Nat. Methods.* 9:671-675.
- Schwab, M., A.S. Lutum, and W. Seufert. 1997. Yeast Hct1 is a regulator of Clb2 cyclin proteolysis. *Cell.* 90:683-693.
- Schwob, E., and K. Nasmyth. 1993. CLB5 and CLB6, a new pair of B cyclins involved in DNA replication in *Saccharomyces cerevisiae*. *Genes & development.* 7:1160-1175.
- Sedgwick, G.G., D.G. Hayward, B. Di Fiore, M. Pardo, L. Yu, J. Pines, and J. Nilsson. 2013. Mechanisms controlling the temporal degradation of Nek2A and Kif18A by the APC/C-Cdc20 complex. *EMBO J.* 32:303-314.
- Shindo, N., K. Kumada, and T. Hirota. 2012. Separase sensor reveals dual roles for separase coordinating cohesin cleavage and cdk1 inhibition. *Dev. Cell.* 23:112-123.
- Shteinberg, M., and A. Hershko. 1999. Role of Suc1 in the activation of the cyclosome by protein kinase Cdk1/cyclin B. *Biochem. Biophys. Res. Commun.* 257:12-18.
- Sigrist, S.J., and C.F. Lehner. 1997. *Drosophila* fizzy-related down-regulates mitotic cyclins and is required for cell proliferation arrest and entry into endocycles. *Cell.* 90:671-681.

- Sikorski, R.S., and P. Hieter. 1989. A system of shuttle vectors and yeast host strains designed for efficient manipulation of DNA in *Saccharomyces cerevisiae*. *Genetics*. 122:19-27.
- Singh, S.A., D. Winter, M. Kirchner, R. Chauhan, S. Ahmed, N. Ozlu, A. Tzur, J.A. Steen, and H. Steen. 2014. Co-regulation proteomics reveals substrates and mechanisms of APC/C-dependent degradation. *EMBO J*. 33:385-399.
- Stegmeier, F., and A. Amon. 2004. Closing mitosis: the functions of the Cdc14 phosphatase and its regulation. *Annu. Rev. Genet.* 38:203-232.
- Straight, A.F., W.F. Marshall, J.W. Sedat, and A.W. Murray. 1997. Mitosis in living budding yeast: anaphase A but no metaphase plate. *Science*. 277:574-578.
- Sullivan, M., L. Holt, and D.O. Morgan. 2008. Cyclin-specific control of ribosomal DNA segregation. *Mol. Cell. Biol.* 28:5328-5336.
- Sullivan, M., and D.O. Morgan. 2007. Finishing mitosis, one step at a time. *Nat. Rev. Mol. Cell Biol.* 8:894-903.
- Tanaka, T., J. Fuchs, J. Loidl, and K. Nasmyth. 2000. Cohesin ensures bipolar attachment of microtubules to sister centromeres and resists their precocious separation. *Nat. Cell Biol.* 2:492-499.
- Tang, Y., and S.I. Reed. 1993. The Cdk-associated protein Cks1 functions both in G₁ and G₂ in *Saccharomyces cerevisiae*. *Genes Dev.* 7:822-832.
- Van Voorhis, V.A., and D.O. Morgan. 2014. Activation of the APC/C ubiquitin ligase by enhanced E2 efficiency. *Current biology*. 24:1556-1562.
- van Zon, W., J. Ogink, B. ter Riet, R.H. Medema, H. te Riele, and R.M.F. Wolthuis. 2010. The APC/C recruits cyclin B1-Cdk1-Cks in prometaphase before D box recognition to control mitotic exit. *J. Cell Biol.* 190:587-602.

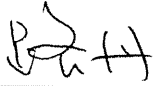
- Vernieri, C., E. Chirolì, V. Francia, F. Gross, and A. Ciliberto. 2013. Adaptation to the spindle checkpoint is regulated by the interplay between Cdc28/Clbs and PP2A^{Cdc55}. *J. Cell Biol.* 202:765-778.
- Visintin, R., S. Prinz, and A. Amon. 1997. CDC20 and CDH1: a family of substrate-specific activators of APC-dependent proteolysis. *Science.* 278:460-463.
- Wang, H., D. Liu, Y. Wang, J. Qin, and S.J. Elledge. 2001. Pds1 phosphorylation in response to DNA damage is essential for its DNA damage checkpoint function. *Genes Dev.* 15:1361-1372.
- Wäsch, R., and F. Cross. 2002. APC-dependent proteolysis of the mitotic cyclin Clb2 is essential for mitotic exit. *Nature.* 418:556-562.
- Wolthuis, R., L. Clay-Farrace, W. van Zon, M. Yekezare, L. Koop, J. Ogink, R. Medema, and J. Pines. 2008. Cdc20 and Cks direct the spindle checkpoint-independent destruction of cyclin A. *Mol. Cell.* 30:290-302.
- Woodbury, E.L., and D.O. Morgan. 2007. Cdk and APC activities limit the spindle-stabilizing function of Fin1 to anaphase. *Nat. Cell Biol.* 9:106-112.
- Yaakov, G., K. Thorn, and D.O. Morgan. 2012. Separase biosensor reveals that cohesin cleavage timing depends on phosphatase PP2A(Cdc55) regulation. *Dev. Cell.* 23:124-136.
- Yang, X., K.Y. Lau, V. Sevim, and C. Tang. 2013. Design principles of the yeast G1/S switch. *PLoS Biol.* 11:e1001673.
- Yeong, F.M., H.H. Lim, C.G. Padmashree, and U. Surana. 2000. Exit from mitosis in budding yeast: biphasic inactivation of the Cdc28-Clb2 mitotic kinase and the role of Cdc20. *Mol. Cell.* 5:501-511.

Publishing Agreement

It is the policy of the University to encourage the distribution of all theses, dissertations, and manuscripts. Copies of all UCSF theses, dissertations, and manuscripts will be routed to the library via the Graduate Division. The library will make all theses, dissertations, and manuscripts accessible to the public and will preserve these to the best of their abilities, in perpetuity.

Please sign the following statement:

I hereby grant permission to the Graduate Division of the University of California, San Francisco to release copies of my thesis, dissertation, or manuscript to the Campus Library to provide access and preservation, in whole or in part, in perpetuity.



Author Signature

12/15/14

Date